



MINISTÉRIO DA CIÊNCIA, TECNOLOGIA, INOVAÇÕES E COMUNICAÇÕES
INSTITUTO NACIONAL DE PESQUISAS ESPACIAIS

sid.inpe.br/mtc-m16c/2019/01.31.14.03-TDI

MODELLING OF THE DIFFUSION FLAME ESTABLISHED AROUND MULTIPLE DROPLETS

Rafael Pereira Bianchin

Master's Dissertation of the Graduate Course in Space Engineering and Technology, guided by Drs. Fernando Fachini Filho, and Cesar Flaubiano da Cruz Cristaldo, approved in February 27, 2019.

URL of the original document:

<<http://urlib.net/8JMKD3MGPDW34P/3SLKLBB>>

INPE
São José dos Campos
2019

PUBLISHED BY:

Instituto Nacional de Pesquisas Espaciais - INPE
Gabinete do Diretor (GBDIR)
Serviço de Informação e Documentação (SESID)
CEP 12.227-010
São José dos Campos - SP - Brasil
Tel.:(012) 3208-6923/7348
E-mail: pubtc@inpe.br

**BOARD OF PUBLISHING AND PRESERVATION OF INPE
INTELLECTUAL PRODUCTION - CEPPII (PORTARIA Nº
176/2018/SEI-INPE):****Chairperson:**

Dr. Marley Cavalcante de Lima Moscati - Centro de Previsão de Tempo e Estudos
Climáticos (CGCPT)

Members:

Dra. Carina Barros Mello - Coordenação de Laboratórios Associados (COCTE)
Dr. Alisson Dal Lago - Coordenação-Geral de Ciências Espaciais e Atmosféricas
(CGCEA)
Dr. Evandro Albiach Branco - Centro de Ciência do Sistema Terrestre (COCST)
Dr. Evandro Marconi Rocco - Coordenação-Geral de Engenharia e Tecnologia
Espacial (CGETE)
Dr. Hermann Johann Heinrich Kux - Coordenação-Geral de Observação da Terra
(CGOBT)
Dra. Ieda Del Arco Sanches - Conselho de Pós-Graduação - (CPG)
Sílvia Castro Marcelino - Serviço de Informação e Documentação (SESID)

DIGITAL LIBRARY:

Dr. Gerald Jean Francis Banon
Clayton Martins Pereira - Serviço de Informação e Documentação (SESID)

DOCUMENT REVIEW:

Simone Angélica Del Ducca Barbedo - Serviço de Informação e Documentação
(SESID)
André Luis Dias Fernandes - Serviço de Informação e Documentação (SESID)

ELECTRONIC EDITING:

Ivone Martins - Serviço de Informação e Documentação (SESID)
Murilo Luiz Silva Gino - Serviço de Informação e Documentação (SESID)



MINISTÉRIO DA CIÊNCIA, TECNOLOGIA, INOVAÇÕES E COMUNICAÇÕES
INSTITUTO NACIONAL DE PESQUISAS ESPACIAIS

sid.inpe.br/mtc-m16c/2019/01.31.14.03-TDI

MODELLING OF THE DIFFUSION FLAME ESTABLISHED AROUND MULTIPLE DROPLETS

Rafael Pereira Bianchin

Master's Dissertation of the Graduate Course in Space Engineering and Technology, guided by Drs. Fernando Fachini Filho, and Cesar Flaubiano da Cruz Cristaldo, approved in February 27, 2019.

URL of the original document:

<<http://urlib.net/8JMKD3MGPDW34P/3SLKLBB>>

INPE
São José dos Campos
2019

Cataloging in Publication Data

Bianchin, Rafael Pereira.

Bi47m Modelling of the diffusion flame established around multiple droplets / Rafael Pereira Bianchin. – São José dos Campos : INPE, 2019.
xx + 63 p. ; (sid.inpe.br/mtc-m16c/2019/01.31.14.03-TDI)

Dissertation (Master in Space Engineering and Technology) – Instituto Nacional de Pesquisas Espaciais, São José dos Campos, 2019.

Guiding : Drs. Fernando Fachini Filho, and Cesar Flaubiano da Cruz Cristaldo.

1. Combustion. 2. Laminar flames. 3. Extinction. I.Title.

CDU 544.452



Esta obra foi licenciada sob uma Licença [Creative Commons Atribuição-NãoComercial 3.0 Não Adaptada](https://creativecommons.org/licenses/by-nc/3.0/).

This work is licensed under a [Creative Commons Attribution-NonCommercial 3.0 Unported License](https://creativecommons.org/licenses/by-nc/3.0/).

Aluno (a): *Rafael Pereira Blanchin*

Título: "MODELLING OF THE DIFFUSION FLAME ESTABLISHED AROUND MULTIPLE DROPLETS"

Aprovado (a) pela Banca Examinadora em cumprimento ao requisito exigido para obtenção do Título de *Mestre* em

Engenharia e Tecnologia Espaciais/Combustão e Propulsão

Dr. Fernando Fachini Filho

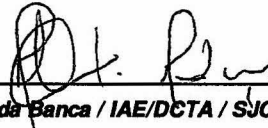


Presidente / Orientador(a) / INPE / Cachoeira Paulista - SP

() *Participação por Vídeo - Conferência*

Aprovado () *Reprovado*

Dr. Márcio Teixeira de Mendonça

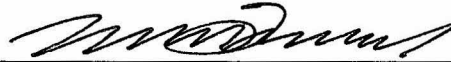


Membro da Banca / IAE/DCTA / SJCampos - SP

() *Participação por Vídeo - Conferência*

Aprovado () *Reprovado*

Dr. Wladimir Mattos da Costa Dourado



Membro da Banca / IAE/DCTA / São José dos Campos - SP

() *Participação por Vídeo - Conferência*

Aprovado () *Reprovado*

Dr. Fernando Marcelo Pereira



Convidado(a) / UFRGS / Porto Alegre - RS

Participação por Vídeo - Conferência

() *Aprovado* () *Reprovado*

Este trabalho foi aprovado por:

() *maioria simples*

unanimidade

“For I know that my redeemer liveth, and that he shall stand at the latter day upon the earth: And though after my skin worms destroy this body, yet in my flesh shall I see God.”

Book of Job 19:25-26

ACKNOWLEDGEMENTS

I am grateful to God who, in his infinite wisdom and mercy, protected and guided me. *We praise thee, O God; we acknowledge thee to be the Lord.*

My sincere thanks to Dr. Fernando Fachini, not only for advising this master thesis but also for the continued partnership and encouragement. I am also grateful to Prof. Cesar Cristaldo.

To my fellow students and colleagues, my most sincere thank you for the friendship.

Mere words would not be enough to express my most profound gratitude to my parents, Valéria and Delcio, and to my siblings, Filipe and Gabriela, whose words could always fill me with faith, hope and love.

This work was supported by grant #1698503, Coordenação de Aperfeiçoamento de Pessoal de Nível Superior (CAPES) and by grant #2017/14758-3, São Paulo Research Foundation (FAPESP).

ABSTRACT

A simplified model for the combustion of multiple droplets is presented under the consideration of unitary Lewis numbers, infinitely fast chemistry and potential flow, and also the assumption that the flame is in the transient region (i.e., sufficiently far from the droplets). The extinction conditions are determined from the Large Activation Energy Asymptotics and studied for several configuration of droplets in axisymmetric geometry. It was found that the critical Damköhler number of extinction decreases monotonically with time, showing that the flame becomes more stable with time. It was also seen that the forced convection makes the flame less stable, but the addition of other droplets does not affect the extinction, which always occur around the largest droplet, unless a smaller droplet is added in the upstream region of a larger droplet, in which case the extinction can occur around the smaller droplet if the convection is sufficiently strong.

Keywords: Combustion; Laminar flames; Extinction.

MODELAGEM DA CHAMA DIFUSIVA ESTABELECIDADA AO REDOR DE MÚLTIPLAS GOTAS

RESUMO

Um modelo simplificado para combustão de múltiplas gotas é apresentado sob a consideração de números de Lewis unitários, química infinitamente rápida e escoamento potencial, e também a consideração de que a chama está na região transiente (isto é, suficientemente longe das gotas). As condições de extinção são determinadas pela Teoria Assintótica de Alta Energia de Ativação e estudada para diversas configurações de gotas em geometria axissimétrica. Foi encontrado que o número de Damköhler crítico de extinção diminui monotonicamente com o tempo, mostrando que a chama fica mais estável com o tempo. Também percebeu-se que a convecção forçada deixa a chama menos estável, mas que a adição de outras gotas não afeta a extinção, que sempre ocorre ao redor da gota maior, a menos que uma gota menor seja adicionada a montante da gota maior. Neste caso, a extinção pode ocorrer ao redor da menor gota se a convecção for suficientemente forte.

Palavras-chave: Chamas laminares; Combustão; Extinção.

LIST OF FIGURES

	<u>Page</u>
3.1 Configuration of the problem for a case with two droplets.	8
3.2 Streamlines for a typical case with two droplets and $V = 1/10$	21
3.3 Solution for Z in the stationary case.	25
3.4 Representation of the numerical domain for a case with two droplets.	28
4.1 Comparison of the flame radius as function of time to an analytical solution for different sizes of the ball in which the boundary condition for the droplets is applied.	29
4.2 Comparison of the flame radius as function of time to the previous results for different sizes of the ball in which the boundary condition for the droplets is applied.	31
5.1 Critical Damköhler number as function of time.	34
5.2 Comparison of the critical Damköhler number to the cases with radiant heat loss. The line continuous represents the result of the current model and the dotted lines represent the results obtained in a previous work.	35
5.3 Distribution of Z for the case without forced convection ($V = 0$) at half the vaporization time ($t = 1/4\beta = 0.0986$). The dashed line represents the flame and the white half circle is the region around the droplet excluded from the domain.	36
5.4 Distribution of Z for the case with convection ($V = 100$) at half the vaporization time ($t = 1/4\beta = 0.0986$).	37
5.5 Critical Damköhler number of extinction along the flame for the case $V = 100$ at half the vaporization time ($t = 1/4\beta = 0.0986$).	37
5.6 Critical Damköhler number of extinction and flame radius as functions of the angle θ for the case $V = 100$ at half the vaporization time ($t = 1/4\beta = 0.0986$).	38
5.7 Maximum critical Damköhler number as function of time for different values of V	39
5.8 Critical Damköhler number along the flame in the moment of merging ($t = 0.0262$) for identical droplets at distance 1.	39
5.9 Critical Damköhler number along the flame in the moment of merging ($t = 0.1012$) for identical droplets at distance 1.5.	40
5.10 Distribution of Z in the moment of merging for identical droplets at distance 1.	40

5.11	Critical Damköhler number as function of time for the cases of a single droplet and of two identical droplets.	41
5.12	Distribution of Z at half the vaporization time ($t = 1/4\beta = 0.0986$) with $V = 100$ and identical droplets at distance 1.	42
5.13	Critical Damköhler number along the flame in the moment of merging ($t = 0.0258$) with $V = 100$ and identical droplets at distance 1.	43
5.14	Critical Damköhler number along the flame at half the vaporization time ($t = 1/4\beta = 0.0986$) with $V = 100$ and identical droplets at distance 1.	44
5.15	Critical Damköhler number of extinction along the flame for two droplets with initial nondimensional radius $a_{01} = 1$ and $a_{02} = 1/2$ at the instant of complete vaporization of the smaller droplet ($t = a_{02}^2/2\beta = 0.050$).	44
5.16	Critical Damköhler number of extinction along the flame for two droplets with initial nondimensional radius $a_{01} = 1$ and $a_{02} = 1/2$ at the instant of complete vaporization of the smaller droplet ($t = a_{02}^2/2\beta = 0.050$) for $V = 100$	45
5.17	Critical Damköhler number of extinction along the flame for two droplets with initial nondimensional radius $a_{01} = 1/2$ and $a_{02} = 1$ at $t = 0.031$ for $V = 150$	46
5.18	Ratio between the critical Damköhler number at the flame in the upstream region of the smaller droplet and in the downstream region (i.e., in the remaining of the domain) as a function of t for different V for the case of two droplets with initial nondimensional radius $a_{01} = 1/2$ and $a_{02} = 1$	47
5.19	Ratio between the critical Damköhler number at the flame in the upstream region of the smaller droplet and in the downstream region (i.e., in the remaining of the domain) as a function of t for different V for the case of two droplets with initial nondimensional radius $a_{01} = 3/4$ and $a_{02} = 1$	48
5.20	Comparison between the distribution of the critical Damköhler number along the flame for the case of identical droplets in steady ambient and the case of different droplets (with initial nondimensional radius $a_{01} = 1/2$ and $a_{02} = 1$) under forced convection with $V = 150$ at $t = 0.020$ and at the instant of merging.	49

LIST OF SYMBOLS

a_i	– nondimensional radius of droplet i
a_{0i}	– nondimensional initial radius of droplet i
\hat{a}_i	– radius of droplet i
\hat{a}_{i0}	– initial radius of droplet i
A_i	– the same as a_{0i}
A_ζ	– parameter in the Large Activation Energy Asymptotics
\hat{B}	– pre-exponential factor
c_p	– nondimensional heat capacity
\hat{c}_p	– heat capacity
$\hat{c}_{p\infty}$	– heat capacity of the ambient
\hat{D}_i	– mass diffusivity of species i
Da	– Damköhler number
Da_E	– critical Damköhler number
\mathbf{e}_{Ri}	– vector pointing away of droplet i
\hat{E}_a	– activation energy
h	– nondimensional enthalpy
\hat{h}	– enthalpy
H	– excess of enthalpy function
\mathcal{H}	– Heaviside step function
\hat{k}	– heat conductivity
K	– constant related to the heat flux from the flame to the fuel region
l	– nondimensional latent heat
\hat{l}	– latent heat
L	– effective Lewis number function
L_r	– size of the numerical domain in r direction
L_z	– size of the numerical domain in z direction
\hat{L}_c	– characteristic length
\hat{L}_{co}	– characteristic length in the transient region
Le_F	– fuel Lewis number
Le_O	– oxidizer Lewis number
N	– number of droplets, also a function in the nonconservative term of the governing equation of H
N_r	– number of points in the r direction
N_z	– number of points in the z direction
q	– nondimensional heat of combustion
\hat{Q}	– heat of combustion
r	– nondimensional radial coordinate in cylindrical coordinates
\mathbf{r}	– nondimensional position vector
r_b	– distance to the droplet in which the boundary condition is applied
\mathbf{r}_k	– position vector of droplet k

$\hat{\mathbf{r}}$	– position vector
\tilde{r}	– nondimensional radial coordinate in spherical coordinates for Section 3.4
R	– nondimensional radial coordinate in spherical coordinates
\hat{R}	– radial coordinate in spherical coordinates
\mathfrak{R}	– gas constant
s	– stoichiometric coefficient
s_H	– constant in the definition of the excess of enthalpy function
s_Z	– nondimensional stoichiometric coefficient
\hat{t}	– time
\hat{t}_c	– characteristic time
t	– nondimensional time
T	– nondimensional temperature
T_a	– nondimensional activation temperature
T_b	– nondimensional boiling temperature of the fuel
T_f	– nondimensional flame temperature
T_o	– nondimensional temperature in the outer zone of the single droplet combustion problem
\hat{T}	– temperature
\hat{T}_b	– fuel boiling temperature
\hat{T}_∞	– ambient temperature
T'^{\pm}	– heat flux from the flame
\mathbf{u}	– nondimensional velocity in the transient region
$\hat{\mathbf{u}}$	– velocity in the transient region
$\hat{\mathbf{u}}_b$	– base flow velocity
u_r	– nondimensional radial velocity in the transient region
u_z	– nondimensional axial velocity in the transient region
U	– nondimensional radial velocity in spherical coordinates
\mathbf{U}	– nondimensional vectorial velocity in the quasi-steady region
\mathbf{U}_i	– nondimensional vectorial velocity generated by droplet i
\hat{U}	– radial velocity in spherical coordinates
y_F	– fuel mass fraction in the transient region
y_O	– oxidizer mass fraction in the transient region
Y_F	– nondimensional fuel mass fraction in the quasi-steady region
\hat{Y}_F	– fuel mass fraction
\hat{Y}_O	– oxidizer mass fraction
$\hat{Y}_{O\infty}$	– ambient oxidizer mass fraction
z	– nondimensional axial coordinate in cylindrical coordinates
z_i	– axial position of the droplet i
Z	– mixture fraction function
α	– nondimensional thermal diffusivity, also, in Section 4, a parameter relating the vaporization time and the extinction time
$\hat{\alpha}_\infty$	– thermal diffusivity of the ambient

β_i	–	vaporization function/constant of droplet i
γ	–	coefficient in the Large Activation Energy Asymptotics
δ	–	reduced Damköhler number, also the Dirac delta function in Appendix A
δ_E	–	critical reduced Damköhler number
Δr	–	mesh resolution in r direction
Δt	–	time step
Δz	–	mesh resolution in z direction
ϵ	–	ratio between gaseous and liquid phase densities
ε	–	small parameter in the Large Activation Energy Asymptotics
ζ	–	independent variable in the Large Activation Energy Asymptotics
θ	–	perturbation of the temperature in the Large Activation Energy Asymptotics
λ_i	–	nondimensional vaporization rate of droplet i
ρ	–	nondimensional density of the gas phase
$\hat{\rho}_l$	–	liquid fuel density
$\hat{\rho}_\infty$	–	gas phase density
ϕ	–	potential function
ϕ_d	–	potential function corresponding to the flow generated by the droplets
ϕ_b	–	potential function of the base flow
Φ	–	generic property
Φ_g	–	generic property in the gas phase
Φ_l	–	generic property in the liquid phase
ψ	–	stream function
ψ_{di}	–	stream function corresponding to the flow generated by droplet i
Ψ_F	–	perturbation of the fuel mass fraction in the Large Activation Energy Asymptotics
Ψ_O	–	perturbation of the oxidizer mass fraction in the Large Activation Energy Asymptotics
χ_f	–	scalar dissipation rate at the flame
ω	–	nondimensional reaction rate
$\hat{\Omega}$	–	reaction rate

CONTENTS

	<u>Page</u>
1 INTRODUCTION	1
2 LITERATURE REVIEW	3
3 METHODOLOGY	7
3.1 Quasi-steady region	8
3.1.1 Boundary conditions at the droplet surface	10
3.1.2 Solution in the gaseous phase	11
3.1.3 Notation for multiple droplets	12
3.2 Transient region	13
3.2.1 Generalized Schvab-Zeldovich formulation	15
3.2.2 Axisymmetric problem	18
3.2.3 Potential flow	19
3.3 Extinction analysis	21
3.3.1 Estimation of the gradient of temperature inside the flame	23
3.4 Regarding the singularity at the droplets	24
3.5 Numerical scheme	26
4 VALIDATION	29
5 RESULTS	33
5.1 Single droplet in steady ambient	33
5.2 Single droplet under forced convection	35
5.3 Pair of identical droplets in steady ambient	38
5.4 Pair of identical droplets under forced convection	42
5.5 Pair of different droplets in steady ambient	43
5.6 Pair of different droplets under forced convection	43
6 CONCLUSIONS	51
6.1 Future work	52

REFERENCES	53
APPENDIX A - AN ALTERNATIVE DERIVATION OF THE BOUNDARY CONDITIONS AT THE DROPLET SURFACE	59
APPENDIX B - THE ASYMPTOTIC STRUCTURE OF DIFFU- SION FLAMES.	61

1 INTRODUCTION

The atomization is related to the burning of liquid fuels in the same way that the heat is related to the combustion. The atomization divides the liquid in small droplets whose total surface is sufficiently large to allow the heat transfer from the ambient to the droplets, allowing a sufficiently large vaporization rate to maintain a flame suitable for the application. The spray is not constituted of droplet of the same size, but rather of a wide spectrum of droplet sizes, which makes the deterministic description of a spray prohibitive, demanding the solution of the Boltzmann equations from the statistic mechanics in nine dimensions to include the time, position, velocity, droplets radius and temperature, and also the description of the base flow, involving the Navier-Stokes and energy conservation equations. A proper description of the dynamics of a spray is of extreme relevance to the achievement of efficiency in combustion.

This master thesis presents a simplified model of the combustion of several droplets developed from the well established models for the combustion of isolated droplets. Suitable methods for the description of the external and internal structure of diffusion flames, with infinitely fast chemistry for the former and finite one-step chemistry for the latter are applied to describe the extinction of the flame around several droplets. One of the applications of the model here presented is in the spray-flamelet model to account for the combustion of small groups of droplets.

The objective of this work is to describe mathematically the flame established around an arbitrary number of droplets, and the specific objectives are to analyze the thermo-fluid-dynamic field around the droplets, to establish the extinction conditions, and to study the influence of a relative flow and the distance and size of the droplets over the extinction.

A review of the literature of droplet interaction is presented in Chapter 2, compiling the most important theoretical, numerical and experimental studies in this theme in the last decades. The mathematical formulation of the combustion of multiple droplets is presented in Chapter 3, describing separately the combustion of isolated droplets, the coupling of the combustion of isolated droplets to the complete problem and the derivation of the extinction conditions for the flame around the droplets. Chapter 4 presents the comparison of the results of the model presented in this master thesis to analytical and numerical results from the literature of combustion of isolated droplets and in Chapter 5 the results obtained with the model are presented and the extinction of the flame is discussed.

2 LITERATURE REVIEW

It is well known that experimental studies with droplets found in Diesel or rocket engines combustion chambers cannot be realized due to their size, which is of order of $10\ \mu\text{m}$. The most usual approach is the use of droplets with size in the order of 1 mm, which are enormous if compared to the actual size of droplets in combustion processes. In those spatial scales the effects of buoyancy deform the flame, which does not happen in droplets in the scale of $10\ \mu\text{m}$, in which case the flame around the droplets is practically spherical. The different flame shape affects the heat flux from the flame to the droplet and, therefore, the vaporization rate is different to the determined for a spherical flame. The solution to this problem is to impose microgravity condition for the large droplets.

In Earth, microgravity can be reached through parabolic flights and drop towers. The first studies employing those methods were in Japan, with prof. Kumagai launching droplet combustion experiments inside a cardboard suitcase from the mechanical engineering building in the University of Tokyo (KUMAGAI; ISODA, 1957). Japan had the largest drop tower, built from a mine shaft approximately 600 m deep. This drop tower was closed due to the large maintenance costs, but there are drop towers nowadays in China, Germany and in the USA. Microgravity can be obtained also with experiments launched from high altitude balloons and orbital flights, although the cost per experiment is very high (NAYAGAM et al., 1998; FACHINI et al., 1999).

Among the studies developed at INPE regarding droplet combustion there are, for example, the effect of the acoustic field over the flame, in which the results showed that the acoustic field anticipates the extinction of the flame around the droplet (FACHINI, 1996). Another issue that was analyzed was the ignition and transient processes around the droplet (FACHINI; LIÑÁN, 1997). It was also studied the transient effects of the acoustic field in the region far of the droplet over the vaporization rate, which had important effects in the flame (FACHINI, 1998). Finally, an analytical model for droplet combustion was developed, which can be implemented in spray combustion simulation codes, for example (FACHINI, 1999).

The interaction between droplets is a natural sequence of the previous studies. The complexity, however is not determined directly by the number of droplets since in this problem the flow field is not one-dimensional anymore, and the velocity is not determined solely by the continuity equation, as in the one-dimensional case of isolated droplets. The following paragraphs do not consist of an extensive discussion of the previous studies on droplet interaction available in the literature, but of a review

of the most relevant studies in the fundamental aspects of droplet interaction, such as the most important theoretical approaches and the numerical and experimental works investigating the differences to the classical case of an isolated droplets. The combustion of sprays is certainly the most studied problem of diffusion flames in theoretical, numerical, and experimental approaches, and the combustion of isolated and interacting droplets is a mere particular case of the combustion of sprays. Therefore, a proper review of the literature of interacting droplets must include the contextualization provided by the combustion of sprays and the intermediate cases that couples the problem of the interaction of a few droplets to the combustion of a cloud of droplets. However, for the sake of brevity, this review will be limited to the problem of the combustion of interacting droplets and arrays of droplets, since there are several review works in the literature dealing with droplet interaction in the context of spray combustion (FAETH, 1977; LAW, 1982; FAETH, 1983; SIRIGNANO, 1983; ANNAMALAI; RYAN, 1992; SIRIGNANO, 2014; SÁNCHEZ et al., 2015).

Three phenomena were identified in the combustion of droplet clouds and sprays, viz., the effect of the droplets in the conditions of the gaseous phase, the effect of the droplets in the local ambient and the effects of the droplets over each other (SIRIGNANO, 1983). Theoretical studies of the burning of interacting droplets were developed to solve the permanent regime problem disregarding the convection, in which case the conservation equations take the form of the Laplace equation, which was approached by numerical methods (LABOWSKY, 1976; LABOWSKY, 1978) and by analytical methods using bispherical coordinates (TWARDUS; BRZUSTOWSKI, 1977; BRZUSTOWSKI et al., 1979). A critical distance between droplets was found such that, if the droplets are closer than that distance, there will be a flame surrounding both droplets. However, it was demonstrated that in most practical applications the droplets are closer than the critical distance and, therefore, combustion of isolated droplets is rare (CHIGIER; MCCREATH, 1974).

Following this theoretical formulation, analytical expressions for the flame shape were obtained, even for the case of different droplets, and it was found that the vaporization rate is smaller for both droplets, although proportional to the case of an isolated droplet (LABOWSKY, 1976). It was also shown that droplet temperatures are independent of the distance between droplets for unitary Lewis numbers (SIRIGNANO, 1983). Further advances to this formulation introduced the effect of convection using potential flow to describe the droplets as point sources (UMEMURA et al., 1981). The Laplace equation formulation was expanded to describe arrays of droplets in different geometries (MARBERRY et al., 1984) which allowed the exten-

sive determination of correction factors for parameters such as the vaporization rate. Studies combining theoretical and experimental analysis showed that droplet interaction increases the burning time and the lifetime of interacting droplets is more than twice larger than of isolated droplets if the distance between droplets is of two diameters (SANGIOVANNI; LABOWSKY, 1982), but that the effects of interaction in the vaporization can be neglected if the distance is larger than 10 diameters.

Later studies took advantage of increasing computational power to expand more convoluted theories for isolated droplets, such as the asymptotic transient behavior of droplets (CRESPO; LIÑÁN, 1975), to the problem of interacting droplets (UMEMURA, 1994), and also the description of the interaction between droplets in the context of dense sprays (SILVERMAN; SIRIGNANO, 1994), revealing that groups of droplets travels in a spray faster than isolated droplets due to the reduction of the drag coefficient, resulting in a shorter droplet lifetime. Complete analysis of the influences the flow over the droplets showed that the assumption of constant distance between droplets is not always accurate and that, under certain conditions, the droplets can collide (CHIANG et al., 1992), even in simple situations such as two droplets with axisymmetry. The effect of forced convection in the burning rates of droplets in axisymmetric geometry were identified (TSAI; STERLING, 1991b), showing that the droplet in the upstream region has a higher burning rate for Reynolds number $Re = 10$ because it is totally enclosed by the flame, while the same happens for $Re = 50$ for the droplets in the downstream region. The use of a potential flow solution for the flow field based on the superposition of point sources to an axial flow was also presented as a suitable alternative to the solution of the Navier-Stokes equations for a system with several droplets (TSAI; STERLING, 1991a), but using the quasi-steady approximation for droplet burning (i.e., solving the governing equations for a stationary solution) as opposed to the model presented in this thesis, in which the solution in the transient region is presented. In the presence of forced convection different flame modes can be observed, such as envelope flame, in which the flame involves the droplet in the upstream region, and the wake flame, in which the flame does not involves the droplet in the upstream region (SIRIGNANO, 2014), and the occurrence of each mode is determined by a critical Damköhler number, which does not depend in the distance between droplets. The flame mode can affect the burning rate of the droplets, since in the wake flame the droplet in the upstream region will have a smaller burning rate.

The combustion of an infinite array of fuel pockets, which can be interpreted as droplets of fuel in a state close to the critical point (i.e., at high temperature and

pressure), was analyzed for different Lewis numbers (CALDEIRA; FACHINI, 2010), showing that the effect of the oxidizer Lewis number on the flame behavior is more relevant because the ambient can provide an unlimited amount of oxidizer to the flame, while the fuel pocket can provide a limited amount of fuel.

The isolated droplet combustion and vaporization models, which has been extensively developed (SAZHIN, 2006), has been used in the modelling of sprays due to its simplicity (MAIONCHI; FACHINI, 2013; FRANZELLI et al., 2015; LIÑÁN et al., 2015), since the quasi-steady regime approximation allows the obtaining of analytical solutions in several cases. The effect of the interaction between droplets on the ignition of sprays was studied, showing that ignition takes more time to occur if the droplets are close to each other in relation to a isolated droplet (SANGIOVANNI; KESTEN, 1977)

Experimental studies performed in several conditions demonstrated the difference to the case of an isolated droplet, such as the fact that interacting droplets no longer follow the d^2 law of vaporization (MIYASAKA; LAW, 1981), but also evidenced the inaccuracy of early theoretical models. It was also shown that the initial distance between droplets affects substantially the vaporization rate, leading to a larger or a smaller vaporization rate in relation to the case of an isolated droplet (MIKAMI et al., 1994). The influence of the pressure over the combustion of interacting droplet was found to be similar to the case of isolated droplets, confirming that the quasi-steady model of droplet combustion is accurate for low pressures (MIKAMI et al., 1998), as predicted much earlier (WILLIAMS, 1960). The effect of the gravity over experimental investigation of the extinction of interacting droplets was found to be relevant, with interacting droplets in normal gravity having the flame extinguished later than isolated droplets and earlier if in microgravity (STRUK et al., 2002), being this phenomena attributed to the radiant heat loss.

This master thesis proposes a model for droplet interaction in which the droplets are far apart. In that case, the flame is in the transient region of droplet combustion, in which the quasi-steady approximation cannot be applied. The conservation equations are solved numerically using the flow field provided by the potential flow instead of the Navier-Stokes equations (TSAI; STERLING, 1991a).

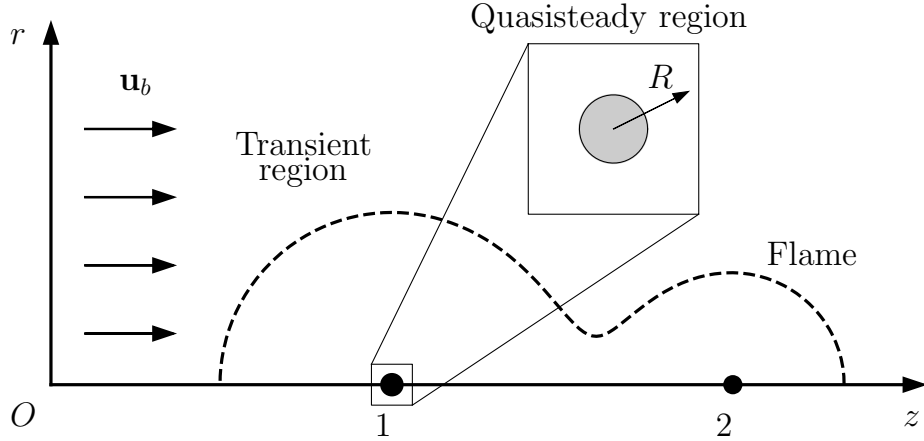
3 METHODOLOGY

The problem consists in a linear array of N droplets of fuel with initial radius \hat{a}_{0k} and density $\hat{\rho}_l$ at boiling temperature \hat{T}_b placed in an ambient of oxidizer with concentration $\hat{Y}_{O\infty}$, temperature \hat{T}_∞ and density $\hat{\rho}_\infty$. There is also an axisymmetric base flow $\hat{\mathbf{u}}_b$. For the sake of simplicity, it is assumed that

- (i) the thermodynamic and transport coefficients are constants;
- (ii) the mass diffusivity of both reactants are equal and equal to their thermal diffusivity (i.e., the Lewis number of both reactants are equal to 1);
- (iii) the density of the gaseous phase is much smaller than the density of the liquid fuel;
- (iv) the chemical reaction is infinitely fast (Burke-Schumann limit), following the one-step mechanism $F + sO_2 \rightarrow (1 + s)P$, in which s is the mass of oxygen required to burn stoichiometrically a unit mass of fuel;
- (v) the problem has axisymmetry around the line passing through the center of the droplets;
- (vi) the flame around the droplets is in the transient region, i.e., the distance from the droplets to the flame is much larger than the droplet radius;
- (vii) the droplets are far from each other (i.e., the distance between the droplets is much larger than their radii), and, therefore, the droplets can be considered as point sources of fuel;
- (viii) the characteristic time of the flow change is much smaller than the characteristic time of energy or species diffusion and convection, so that the flow is stationary in relation to the other variables;
- (ix) in addition to being stationary, the flow is incompressible and irrotational and, therefore, potential.

The problem will be described in cylindrical coordinates, in which the axis z pass through the center of the droplets and the axis r is perpendicular to z . This configuration for a case with two droplets is depicted in Fig. (3.1).

Figure 3.1 - Configuration of the problem for a case with two droplets.



After the ignition of the flame around a droplet the steady state in the region immediately close to the droplet is rapidly achieved, and transient effects are relevant mainly far from the droplet (CRESPO; LIÑÁN, 1975). The region close to the droplet, called quasisteady region, is not affected by the external problem and can therefore be solved separately. The region far from the droplet, called transient region, will be solved as a single phase problem, in which the presence of droplets is regarded through boundary conditions obtained by the analysis in the quasisteady region. Since in the quasisteady region the droplet can be assumed to be isolated, the problem in this scale is one-dimensional and can be described by the radial variable $R = \sqrt{(r^2 + (z - z_d)^2)/\epsilon}$, in which z_d is the position of the droplet and ϵ is a scale factor to be defined later.

3.1 Quasi-steady region

Initially, the combustion of an isolated droplet with initial radius \hat{a}_0 is addressed, which will provide the boundary condition that represents the droplet as a point source of fuel. It is assumed that the density and the thermodynamic and transport coefficients are constant in both gaseous and liquid phase, although they are kept in the equations to address the difference of these properties in each phase. It is assumed also that the problem of the combustion of a single droplet has spherical symmetry, with \hat{R} being the radial coordinate with origin in the center of the droplet and \hat{U} being the radial velocity. Since the flame is assumed to be in the transient region the oxidizer concentration in the quasi-steady region is 0 and, therefore, only the fuel conservation equation will be written. The conservation equations are the

continuity equation

$$\frac{\partial \hat{\rho}}{\partial \hat{t}} + \frac{1}{\hat{R}^2} \frac{\partial}{\partial \hat{R}} (\hat{R}^2 \hat{\rho} \hat{U}) = 0, \quad (3.1)$$

the energy conservation equation (in terms of the enthalpy $\hat{h} = \hat{c}_p \hat{T}$),

$$\frac{\partial(\hat{\rho} \hat{h})}{\partial \hat{t}} + \frac{1}{\hat{R}^2} \frac{\partial}{\partial \hat{R}} (\hat{R}^2 \hat{\rho} \hat{U} \hat{h}) = \frac{1}{\hat{R}^2} \frac{\partial}{\partial \hat{R}} \left(\hat{R}^2 \hat{k} \frac{\partial \hat{T}}{\partial \hat{R}} \right), \quad (3.2)$$

and the fuel conservation equation,

$$\frac{\partial(\hat{\rho} \hat{Y}_F)}{\partial \hat{t}} + \frac{1}{\hat{R}^2} \frac{\partial}{\partial \hat{R}} (\hat{R}^2 \hat{\rho} \hat{U} \hat{Y}_F) = \frac{1}{\hat{R}^2} \frac{\partial}{\partial \hat{R}} \left(\hat{R}^2 \hat{\rho} \hat{D}_F \frac{\partial \hat{Y}_F}{\partial \hat{R}} \right). \quad (3.3)$$

Defining the nondimensional independent variables (i.e., time and radial coordinate)

$$t := \frac{\hat{t}}{\hat{t}_c}, \quad R := \frac{\hat{R}}{\hat{L}_c} \quad (3.4)$$

the nondimensional dependent variables density ρ , enthalpy h , temperature T , fuel mass fraction Y_F , and radial velocity U

$$\rho := \frac{\hat{\rho}}{\hat{\rho}_\infty}, \quad h := \frac{\hat{h}}{\hat{c}_p \hat{T}_\infty}, \quad T := \frac{\hat{T}}{\hat{T}_\infty}, \quad Y_F := \hat{Y}_F, \quad U := \frac{\hat{t}_c \epsilon}{\hat{L}_c} \hat{U}, \quad (3.5)$$

and the thermal diffusivity

$$\alpha := \frac{\hat{k}}{\hat{c}_p \hat{\rho}_\infty} \quad (3.6)$$

in which the characteristic time is $\hat{t}_c := \hat{a}_0^2 / \hat{\alpha}_\infty \epsilon$, i.e., the time scale corresponding to the droplet heating and vaporization, and the characteristic length is $\hat{L}_c := \hat{a}_0$, the initial droplet radius, with $\epsilon := \hat{\rho}_\infty / \hat{\rho}_l$ (CRESPO; LIÑÁN, 1975). The nondimensional equations are, therefore,

$$\epsilon \frac{\partial \rho}{\partial t} + \frac{1}{R^2} \frac{\partial}{\partial R} (R^2 \rho U) = 0 \quad (3.7)$$

$$\epsilon \frac{\partial(\rho h)}{\partial t} + \frac{1}{R^2} \frac{\partial}{\partial R} (R^2 \rho U h) = \frac{1}{R^2} \frac{\partial}{\partial R} \left(R^2 \alpha \frac{\partial T}{\partial R} \right), \quad (3.8)$$

$$Le_F \left[\epsilon \frac{\partial(\rho Y_F)}{\partial t} + \frac{1}{R^2} \frac{\partial}{\partial R} (R^2 \rho U Y_F) \right] = \frac{1}{R^2} \frac{\partial}{\partial R} \left(R^2 \rho \alpha \frac{\partial Y_F}{\partial R} \right), \quad (3.9)$$

in which the Lewis number of the fuel is given by

$$Le_F := \frac{\hat{\alpha}_\infty}{\hat{D}_{F\infty}}. \quad (3.10)$$

It must be pointed out that

$$\rho = c_p = \alpha = 1 \quad (3.11)$$

in the gaseous phase and that

$$\rho = \rho_l = \epsilon^{-1}, \quad c_p = c_{pl}, \quad \alpha = \alpha_l \quad (3.12)$$

in the liquid phase (consid. (i)). It can be seen that ϵ is the Strouhal number, which is the ratio of the characteristic time scale of the gaseous phase to the characteristic time scale of the liquid phase.

3.1.1 Boundary conditions at the droplet surface

The boundary conditions at the droplet surface are provided by the integration of the conservation equations across the droplet surface. The integration of the continuity equation leads to

$$0 = R^2 \rho U \Big|_{a^-}^{a^+} = a^2 \rho U - a^2 \epsilon^{-1} U_r = a^2 \rho U + a^2 \frac{da}{dt} = a^2 \rho U - \lambda, \quad (3.13)$$

in which $U_r = -\epsilon da/dt$ is the velocity of regression of the droplet surface and λ is the nondimensional vaporization rate, given by

$$\lambda := -a^2 \frac{da}{dt} = -\frac{d}{dt} \left(\frac{1}{3} a^3 \right) \quad (3.14)$$

which, apart of a factor of 4π , is the rate of change of the droplet mass. Therefore, the continuity equation leads to

$$a^2 \rho U = \lambda. \quad (3.15)$$

Using $\lambda/a = -da^2/dt$, the droplet radius can be written as function of λ as

$$a^2 = 1 - 2 \int_0^t \frac{\lambda}{a} dt. \quad (3.16)$$

Integrating the energy conservation equation, one has

$$R^2 \rho U h \Big|_{a^-}^{a^+} = R^2 \alpha \frac{\partial T}{\partial R} \Big|_{a^-}^{a^+}, \quad (3.17)$$

or, since the temperature distribution is assumed to be uniform inside the droplet,

$$\lambda h|_{a^-}^{a^+} = a^2 \frac{\partial T}{\partial R} \Big|_{a^+}. \quad (3.18)$$

The term in the left-hand side is the difference of the enthalpy of the liquid and the gaseous phases. Since the fuel in the droplet is at boiling temperature, this difference is the latent heat of vaporization $l := \hat{l}/\hat{c}_{p\infty}\hat{T}_\infty$. Therefore,

$$a^2 \frac{\partial T}{\partial R} \Big|_{a^+} = \lambda l. \quad (3.19)$$

The integration of the fuel conservation equation leads to

$$a^2 \frac{\partial Y_F}{\partial R} \Big|_{a^+} - Le_F \lambda Y_F = -Le_F \lambda. \quad (3.20)$$

An alternative derivation of these boundary conditions is presented in Appendix A.

3.1.2 Solution in the gaseous phase

The conservation equations can be integrated in the gaseous phase evaluating the integrals in the region $R > a$. Under the assumption that $\epsilon \ll 1$ (consid. (v)) the transient term will be neglected. From henceforth it will be assumed that the specific heat of the gaseous phase is constant (consid. (i)), with $c_p = 1$, leading to $h = T$. The integration of the continuity equation leads to

$$U = \frac{\lambda}{R^2}. \quad (3.21)$$

For the energy conservation equation,

$$R^2 \frac{dT}{dR} \Big|_a^R = R^2 UT \Big|_a^R, \quad (3.22)$$

leading to

$$R^2 \frac{dT}{dR} = \lambda(T - T_b + l), \quad (3.23)$$

in which T_b is the boiling temperature, that can be assumed as identical to the temperature of the droplet surface (WILLIAMS, 1985; LAW, 2006). For the fuel conservation equation,

$$R^2 \frac{dY_F}{dR} = Le_F \lambda (Y_F - 1). \quad (3.24)$$

These equations can be written in a more compact form as

$$\frac{\lambda}{R^2} = \frac{1}{T - T_b + l} \frac{dT}{dR} = \frac{1}{Le_F(Y_F - 1)} \frac{dY_F}{dR}. \quad (3.25)$$

Integrating these equations, one has

$$\exp\left(-\frac{\lambda}{R}\right) = \frac{T - T_b + l}{T_o - T_b + l} = \left(\frac{Y_F - 1}{Y_{F_o} - 1}\right)^{1/Le_F}, \quad (3.26)$$

in which the subscript o stands for the condition in the outer zone (i.e., in the limit $R \rightarrow \infty$). The first equality can be applied to $R = a$, yielding

$$\frac{\lambda}{a} = \beta(t) := \ln\left(1 + \frac{T_o - T_b}{l}\right), \quad (3.27)$$

in which β is the vaporization function, which is a function of time through the dependence of T_o on time. Therefore, the droplet radius can be obtained by

$$a^2 = 1 - 2 \int_0^t \beta dt. \quad (3.28)$$

In the classical theory of droplet combustion, β is a constant (called vaporization constant) because the temperature around the droplet is constant, as it will be demonstrated in Section 3.2.1. Under this condition one has $a^2 = 1 - 2\beta t$, i.e., the square of the droplet radius decreases linearly with time, as stated by the d^2 law (GODSAVE, 1953; SPALDING, 1953).

3.1.3 Notation for multiple droplets

Since the problem will be addressed with an arbitrary number of droplets, the notation must be accordingly expanded. The subscript k will denote the properties of the k -th droplet, e.g., λ_k is the vaporization rate of droplet k . Droplet 1 has initial radius \hat{a}_{01} , and droplet k has initial radius $\hat{a}_{0k} = A_k \hat{a}_{01}$. Evaluating the nondimensionalization with the initial radius of droplet 1 has no effect on the formulation except that the radius of droplet k as function of vaporization function β_k is

$$a_k^2 = A_k^2 - 2 \int_0^t \beta_k dt. \quad (3.29)$$

3.2 Transient region

In the description of the gas phase far from the droplet, called outer problem, the geometry of the droplets is not seen (consid. (vi)). It is assumed that N droplets are placed at $\hat{\mathbf{r}} = \hat{\mathbf{r}}_k$, $k = 1, 2, \dots, N$.

The conservation equations in the transient region are

$$\nabla \cdot \hat{\mathbf{u}} = 0, \quad (3.30)$$

$$\frac{\partial \hat{T}}{\partial \hat{t}} + \nabla \cdot (\hat{\mathbf{u}} \hat{T}) = \hat{\alpha} \nabla^2 \hat{T} + \hat{Q} \hat{\omega}, \quad (3.31)$$

$$\frac{\partial \hat{Y}_O}{\partial \hat{t}} + \nabla \cdot (\hat{\mathbf{u}} \hat{Y}_O) = \hat{\mathcal{D}}_O \nabla^2 \hat{Y}_O - s \hat{\omega}, \quad (3.32)$$

$$\frac{\partial \hat{Y}_F}{\partial \hat{t}} + \nabla \cdot (\hat{\mathbf{u}} \hat{Y}_F) = \hat{\mathcal{D}}_F \nabla^2 \hat{Y}_F - \hat{\omega}, \quad (3.33)$$

in which $\hat{\omega}$ is the reaction rate for a one-step mechanism (consid. (iii)), given by

$$\hat{\omega} = \hat{B} \hat{Y}_O \hat{Y}_F \exp\left(-\frac{\hat{E}_a}{\mathfrak{R} \hat{T}}\right), \quad (3.34)$$

in which \hat{B} is the pre-exponential factor, \hat{E}_a is the activation energy and \mathfrak{R} is the gas constant.

The proper length scale in the outer problem is $\hat{L}_{co} := \hat{\alpha}_{01} / \sqrt{\epsilon}$ (CRESPO; LIÑÁN, 1975; WALDMAN, 1975). The nondimensional variables of the outer zone are therefore

$$\mathbf{r} := \frac{\hat{\mathbf{r}}}{\hat{L}_{co}}, \quad \mathbf{u} := \frac{\hat{t}_c}{\hat{L}_{co}} \hat{\mathbf{u}}, \quad y_O := \frac{\hat{Y}_O}{\hat{Y}_{O\infty}}, \quad y_F := \frac{\hat{Y}_F}{\sqrt{\epsilon}}, \quad (3.35)$$

while the remaining variables are the same of the quasisteady region (Eq. (3.5)). The outer zone variables are related to the inner zone variables by (CRESPO; LIÑÁN, 1975; WALDMAN, 1975; FACHINI et al., 1999)

$$\mathbf{r} = \sqrt{\epsilon}(\mathbf{R} - \mathbf{R}_0), \quad \mathbf{u} = \frac{\mathbf{U}}{\sqrt{\epsilon}}, \quad y_F = \frac{Y_F}{\sqrt{\epsilon}}, \quad (3.36)$$

in which \mathbf{R} and \mathbf{U} are the position and velocity vector in the inner zone, respectively, and \mathbf{R}_0 allows an arbitrary translation of the origin. The nondimensional conservation equations are

$$\nabla \cdot \mathbf{u} = 0, \quad (3.37)$$

$$\frac{\partial T}{\partial t} + \nabla \cdot (\mathbf{u}T) = \nabla^2 T + q\omega, \quad (3.38)$$

$$Le_O \left[\frac{\partial y_O}{\partial t} + \nabla \cdot (\mathbf{u}y_O) \right] = \nabla^2 y_O - s_Z \omega, \quad (3.39)$$

$$Le_F \left[\frac{\partial y_F}{\partial t} + \nabla \cdot (\mathbf{u}y_F) \right] = \nabla^2 y_F - \omega, \quad (3.40)$$

in which the nondimensional reaction rate is given by

$$\omega = Da y_O y_F \exp \left[\frac{T_a}{T_f} \left(1 - \frac{T_f}{T} \right) \right], \quad (3.41)$$

in which $T_a := \hat{E}_a / \mathfrak{R} \hat{T}_\infty$ is the nondimensional activation temperature, often identified as Zeldovich number, and T_f is nondimensional flame temperature. The Lewis numbers of the oxidizer are given by, respectively,

$$Le_O := \frac{\hat{\alpha}}{\mathcal{D}_O}, \quad Le_F := \frac{\hat{\alpha}}{\mathcal{D}_F}, \quad (3.42)$$

and the nondimensional heat of combustion (q), the Damköhler number (Da) and the stoichiometric coefficient s_Z are given by

$$q := \sqrt{\epsilon} \frac{\hat{Q}}{\hat{c}_p \hat{T}_\infty Le_F}, \quad Da = \hat{Y}_{O_\infty} Le_F \frac{\hat{\alpha}_0^2 \hat{B} e^{-T_a/T_f}}{\epsilon \hat{\alpha}_\infty}, \quad s_Z = \sqrt{\epsilon} \frac{s Le_O}{\hat{Y}_{O_\infty} Le_F}. \quad (3.43)$$

The results obtained for the quasisteady region (i.e., Eq. (3.26)) can be written in terms of the outer zone variables as

$$\|\mathbf{r} - \mathbf{r}_k\|^2 \nabla T \cdot \mathbf{e}_{Rk} = \sqrt{\epsilon} \lambda_k (T - T_b + l), \quad (3.44)$$

$$\frac{\|\mathbf{r} - \mathbf{r}_k\|^2}{Le_O} \nabla y_O \cdot \mathbf{e}_{Rk} = \sqrt{\epsilon} \lambda_k y_O, \quad (3.45)$$

$$\frac{\|\mathbf{r} - \mathbf{r}_k\|^2}{Le_F} \nabla y_F \cdot \mathbf{e}_{Rk} = -\lambda_k, \quad \mathbf{r} \rightarrow \mathbf{r}_k, \quad (3.46)$$

in which $\mathbf{e}_{Rk} := (\mathbf{r} - \mathbf{r}_k) / \|\mathbf{r} - \mathbf{r}_k\|$ is the unit vector pointing away from the droplet k center. In the boundary condition for y_F it was assumed that $\sqrt{\epsilon} y_F \ll 1$. These boundary conditions can be interpreted as point sources of fuel and sinks of energy at the droplets (consid. (vii)). The initial conditions can be chosen as

$$T = 1, \quad y_O = 1, \quad y_F = 0, \quad (3.47)$$

which represents an initially uniform ambient of oxidizer.

3.2.1 Generalized Schvab-Zeldovich formulation

If the chemical reaction is much faster than the transport processes the reaction is confined to a thin region, outside of which the flow is inert (consid. (iii)). This situation is reflected in the reaction term (Eq. (3.41)), since the Damköhler number Da is the ratio between the diffusion characteristic time $\hat{t}_c = \hat{a}_0^2/\epsilon\hat{\alpha}_\infty$ and the reaction characteristic time $\hat{B}^{-1}e^{T_a/T_f}$. In the limit $Da \rightarrow \infty$ (i.e., the reaction time is much smaller than the diffusion time) the reaction term is not infinite only if $y_F y_O \rightarrow 0$, i.e., if the reactants do not coexist.

In the present case, the fuel is provided by droplets in $\mathbf{r} = \mathbf{r}_k$ and the oxidizer by the ambient ($\|\mathbf{r}\| \rightarrow \infty$). Therefore, the flame is confined to a reaction sheet, i.e., a closed surface, inside of which $y_O = 0$ and $y_F > 0$ and outside of which $y_O > 0$ and $y_F = 0$. On that surface, both y_O and y_F are 0. Since the reactants do not coexist, a variable Z (called mixture fraction) can be defined combining y_O and y_F and taking advantage of the linearity of the equations to suppress the reaction term of the governing equation of Z . Defining Z as

$$Z := s_Z y_F - y_O + 1 \quad (3.48)$$

one has (LIÑÁN, ; LIÑÁN; WILLIAMS, 1993; FACHINI et al., 1999; LIÑÁN, 2001)

$$L(Z) \left(\frac{\partial Z}{\partial t} + \nabla \cdot (\mathbf{u}Z) \right) = \nabla^2 Z, \quad (3.49)$$

in which $L(Z)$ is the effective Lewis number, a discontinuous function defined as

$$L(Z) := \begin{cases} Le_F, & Z > 1 \\ Le_O, & Z < 1. \end{cases} \quad (3.50)$$

Since in the flame $y_O = y_F = 0$, the flame can be defined as the surface corresponding to $Z = 1$. The region in which $Z > 1$ corresponds to the fuel region and the region in which $0 < Z < 1$ corresponds to the oxidizer region.

In a similar fashion, defining the excess enthalpy H as

$$H := s_H T + y_O + y_F, \quad (3.51)$$

with $s_H := (s_Z + 1)/q$, one has

$$\frac{\partial H}{\partial t} + \nabla \cdot (\mathbf{u}H) = \nabla^2 H + N(Z)\nabla^2 Z, \quad (3.52)$$

in which $N(Z)$ is defined as

$$N(Z) := \begin{cases} (1 - Le_F)/s_Z Le_F, & Z > 1 \\ (Le_O - 1)/Le_O, & Z < 1. \end{cases} \quad (3.53)$$

The equations for Z and H can also be written in conservative form as

$$\left(\frac{\partial}{\partial t} + \nabla \cdot \mathbf{u} \right) \int_1^Z L(\zeta) d\zeta = \nabla^2 Z, \quad (3.54)$$

$$\left(\frac{\partial}{\partial t} + \nabla \cdot \mathbf{u} \right) H = \nabla^2 H + \nabla^2 \int_1^Z N(\zeta) d\zeta. \quad (3.55)$$

The integrals $\int_1^Z L d\zeta$ and $\int_1^Z N d\zeta$ can be identified with the functions G and K defined by Liñán (LIÑÁN,), respectively.

Although there are several effects associated with the difference between the Lewis number of the reactants (ALMAGRO et al., 2018), the use of $Le_O \neq Le_F$ leads to critical difficulties due to the fact that the function Z is no longer suitable to fulfill the role of a independent variable (CHEATHAM; MATALON, 2000), as is required by the flamelet formulation (PETERS, 1983), which will be introduced in Section 3.3, due to the fact that the existence of a bijection between Z and T , for example, is no longer assured. Since the introduction of the flamelet formulation is necessary to evaluate the extinction conditions in a diffusion flame following the classical Large Activation Energy Asymptotics (LIÑÁN, 1974), it will be assumed hereinafter that $Le_O = Le_F = 1$. In future developments over this theme the effects of differential diffusion in the extinction of the flame will be addressed through the application of suitable methods (CHEATHAM; MATALON, 2000; LIÑÁN et al., 2017). With the consideration $Le_O = Le_F = 1$ (consid. (ii)), the equations for Z and H are reduced to

$$\frac{\partial Z}{\partial t} + \nabla \cdot (\mathbf{u}Z) = \nabla^2 Z, \quad (3.56)$$

$$\frac{\partial H}{\partial t} + \nabla \cdot (\mathbf{u}H) = \nabla^2 H, \quad (3.57)$$

with initial conditions

$$Z = 0, \quad H = s_H + 1, \quad (3.58)$$

and the boundary conditions are: far from the droplets,

$$Z = 0, \quad H = s_H + 1, \quad \|\mathbf{r}\| \rightarrow \infty, \quad (3.59)$$

and at the droplets,

$$\|\mathbf{r} - \mathbf{r}_k\|^2 \nabla Z \cdot \mathbf{e}_{Rk} = -s_Z \lambda_k, \quad (3.60)$$

$$\|\mathbf{r} - \mathbf{r}_k\|^2 \nabla H \cdot \mathbf{e}_{Rk} = -\lambda_k \left[1 - \sqrt{\epsilon} \left(H - \frac{Z - 1}{s_Z} - s_H (T_b - l) \right) \right], \quad \mathbf{r} \rightarrow \mathbf{r}_k. \quad (3.61)$$

The boundary conditions in the droplets can be interpreted as point sources of fuel and sinks of energy. The boundary condition for y_O at the droplets was eliminated because the flame always surrounds the droplets, preventing the oxidizer to reach it.

In the limit of small $\sqrt{\epsilon}$ the boundary condition for H at the droplets can be simplified to

$$\|\mathbf{r} - \mathbf{r}_k\|^2 \nabla H \cdot \mathbf{e}_{Rk} = -\lambda_k. \quad (3.62)$$

In that case Z and H are not linearly independent, which can be proved defining the function $J := H - Z/s_Z - (s_H + 1)$ (FACHINI et al., 1999), whose governing equation is

$$\frac{\partial J}{\partial t} + \nabla \cdot (\mathbf{u}J) = \nabla^2 J, \quad (3.63)$$

and whose boundary conditions are

$$J = 0, \quad \|\mathbf{r}\| \rightarrow \infty, \quad (3.64)$$

$$\|\mathbf{r} - \mathbf{r}_k\|^2 \nabla J \cdot \mathbf{e}_{Rk} = 0, \quad \mathbf{r} \rightarrow \mathbf{r}_k. \quad (3.65)$$

and with initial condition $J = 0$. Therefore, from the maximum principle for parabolic equations $J \equiv 0$ in the entire domain for all $t \geq 0$ (PROTTER; WEINBERGER, 2012), and then H can be written as function of Z as

$$H = \frac{Z}{s_Z} + s_H + 1. \quad (3.66)$$

From the definition of Z and H (Eqs. (3.48) and (3.51), respectively), one has

$$T = 1 + \frac{s_Z + 1}{s_Z s_H} = 1 + \frac{q}{s_Z}, \quad Z > 1, \quad (3.67)$$

i.e., the temperature is constant inside the flame, and

$$T = 1 + \frac{q}{s_Z} Z, \quad Z < 1, \quad (3.68)$$

i.e., outside the flame. Therefore, the flame temperature (i.e., for $Z = 1$) is

$$T_f = 1 + \frac{q}{s_Z}. \quad (3.69)$$

Also, in this limit, since the temperature is constant around the droplets, the vaporization function β is constant (vid. Eq. (3.27)), given by

$$\beta = \ln \left(1 + \frac{T_f - T_b}{l} \right), \quad (3.70)$$

and Eq. (3.28) can be readily integrated, leading to

$$a_k = \sqrt{A_k^2 - 2\beta t}, \quad (3.71)$$

showing that the droplets radii follow the d^2 law.

The extinction analysis requires the determination of the gradient of temperature in both sides of the flame. Since the limit of small $\sqrt{\epsilon}$ leads to constant T inside the flame (in which case the flame cannot be extinguished), it is inappropriate to use this simplification. However, the d^2 law will still be used for the sake of simplicity.

3.2.2 Axisymmetric problem

With the assumption that all the droplets lie in the same axis the equations can be written in cylindrical coordinates with axisymmetry (consid. (iv)). The axial coordinate z is defined by the axis passing through the droplets and the radial coordinate r is perpendicular to z . In that case $\mathbf{r} = r\mathbf{e}_r + z\mathbf{e}_z$, $\mathbf{u} = u_r\mathbf{e}_r + u_z\mathbf{e}_z$, and the equations are

$$\frac{\partial Z}{\partial t} + \frac{\partial}{\partial r}(u_r Z) + \frac{\partial}{\partial z}(u_z Z) = \frac{1}{r} \frac{\partial}{\partial r} \left(r \frac{\partial Z}{\partial r} \right) + \frac{\partial^2 Z}{\partial z^2}, \quad (3.72)$$

$$\frac{\partial H}{\partial t} + \frac{\partial}{\partial r}(u_r H) + \frac{\partial}{\partial z}(u_z H) = \frac{1}{r} \frac{\partial}{\partial r} \left(r \frac{\partial H}{\partial r} \right) + \frac{\partial^2 H}{\partial z^2}, \quad (3.73)$$

and the boundary conditions are: at the symmetry axis,

$$\frac{\partial Z}{\partial r} = \frac{\partial H}{\partial r} = 0, \quad r = 0, \quad (3.74)$$

far from the droplets,

$$Z = 0, \quad H = s_H + 1, \quad r, z \rightarrow \infty, \quad (3.75)$$

and at the droplets

$$\sqrt{r^2 + (z - z_k)^2} \left(r \frac{\partial Z}{\partial r} + (z - z_k) \frac{\partial Z}{\partial z} \right) = -s_Z \lambda_k, \quad (3.76)$$

$$\begin{aligned} & \sqrt{r^2 + (z - z_k)^2} \left(r \frac{\partial H}{\partial r} + (z - z_k) \frac{\partial H}{\partial z} \right) = \\ & -\lambda_k \left[1 - \sqrt{\epsilon} \left(H - \frac{Z - 1}{s_Z} - s_H(T_b - l) \right) \right], \quad r \rightarrow 0, \quad z \rightarrow z_k, \end{aligned} \quad (3.77)$$

in which z_k is the position of the droplet k along the z axis.

3.2.3 Potential flow

The existence of a potential function ϕ such that $\mathbf{u} = \nabla\phi$ ensures that the continuity equation $0 = \nabla \cdot \mathbf{u} = \nabla^2\phi$ is satisfied as long as ϕ is a harmonic function, i.e., a solution to the Laplace equation. The linearity of the Laplace equation allows the superposition of different potential functions to describe a flow (KUNDU; COHEN, 2004).

It is assumed that the flow consists in the superposition of the flow caused by the droplets ($\nabla\phi_d$) on a base ($\nabla\phi_b$) flow, i.e., $\phi = \phi_d + \phi_b$, in which ϕ_d itself is the superposition of the flow generated by all the droplets. The velocity field generated by each droplet, given by Eq. (3.21), can be written in vectorial form as

$$\mathbf{U}_k = \frac{\lambda_k}{\|\mathbf{R}_k\|^2} \mathbf{e}_{Rk}, \quad (3.78)$$

or, in outer zone coordinates,

$$\mathbf{u}_k = \frac{\sqrt{\epsilon}\lambda_k}{\|\mathbf{r} - \mathbf{r}_k\|^2} \mathbf{e}_{Rk} = \frac{\sqrt{\epsilon}\lambda_k}{(r^2 + (z - z_k)^2)^{3/2}} [r\mathbf{e}_r + (z - z_k)\mathbf{e}_z]. \quad (3.79)$$

It can be seen that one has $\|\mathbf{u}_k\| \sim 1$ for $\|\mathbf{r} - \mathbf{r}_k\| \sim \epsilon^{1/4}\lambda_k^{1/2}$. Assuming that the vaporization rate is of order unity, the distance affected by the convection of fuel from the droplet is of order $\epsilon^{1/4}$.

Since \mathbf{u}_k depends on time due to λ , there is no potential function such that $\mathbf{u}_k = \nabla\phi_{dk}$. However, it is assumed that the characteristic time of flow change is much

smaller than the characteristic time of convection and diffusion, and therefore the flow can be considered to be quasisteady (consid. (viii)). The potential function associated with the field generated by the droplets is then (consid. (ix))

$$\phi_d = -\sqrt{\epsilon} \sum_k \frac{\lambda_k}{\sqrt{r^2 + (z - z_k)^2}}. \quad (3.80)$$

The base flow is assumed to be a uniform flow of intensity $\sqrt{\epsilon}V$ in the axial direction (with $V := \hat{t}_c/\hat{a}_{01}\hat{V}$, in which \hat{V} is the dimensional magnitude of the axial velocity), whose potential function is $\phi_b = \sqrt{\epsilon}Vz$, preserving the axisymmetry of the problem. Therefore, the potential function is

$$\phi = \sqrt{\epsilon} \left(Vz - \sum_k \frac{\lambda_k}{\sqrt{r^2 + (z - z_k)^2}} \right) \quad (3.81)$$

and the velocity components are

$$u_r = \sqrt{\epsilon} \sum_k \frac{r}{(r^2 + (z - z_k)^2)^{3/2}} \lambda_k, \quad (3.82)$$

$$u_z = \sqrt{\epsilon} \left(V + \sum_k \frac{(z - z_k)}{(r^2 + (z - z_k)^2)^{3/2}} \lambda_k \right). \quad (3.83)$$

For axisymmetric flow the streamfunction ψ must satisfy $\mathbf{u} = -\nabla\phi \times \nabla\psi$ (KUNDU; COHEN, 2004). The streamfunction corresponding to the uniform flow is $\psi_b = \sqrt{\epsilon}Vr^2/2$ and the streamfunction corresponding to each droplet is

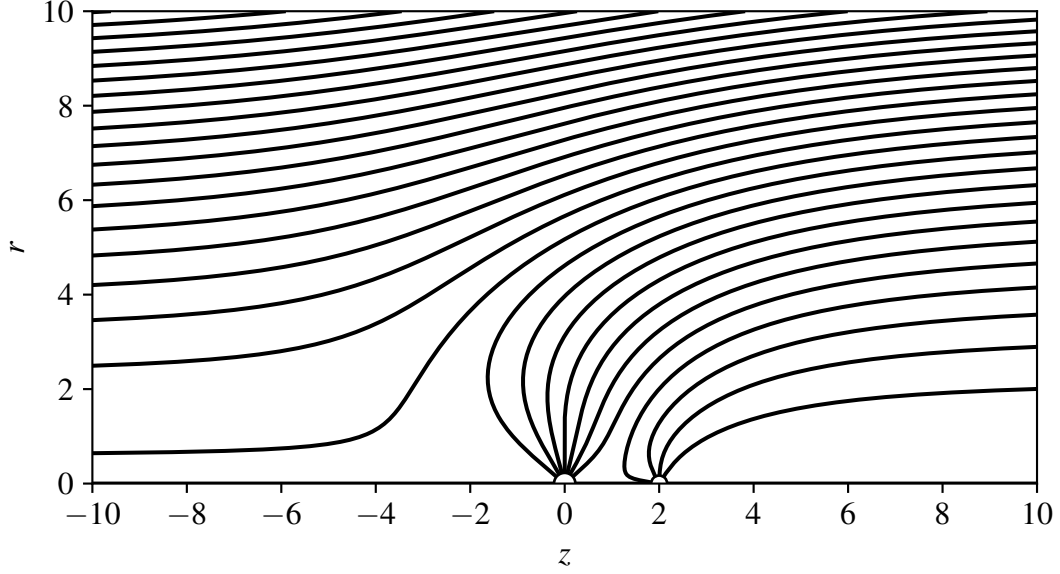
$$\psi_{dk} = -\sqrt{\epsilon} \frac{z - z_k}{\sqrt{r^2 + (z - z_k)^2}} \lambda_k. \quad (3.84)$$

Therefore, the complete streamfunction is

$$\psi = \sqrt{\epsilon} \left(\frac{1}{2}Vr^2 - \sum_k \frac{z - z_k}{\sqrt{r^2 + (z - z_k)^2}} \lambda_k \right). \quad (3.85)$$

The contours of ψ , i.e., the streamlines, are shown in Fig. (3.2) for a case with two droplets placed at $z = 0$ and $z = 2$, being the former twice as larger than the latter, and $V = 1/10$. The markers corresponds to the droplets positions, but their sizes does not correspond to the sizes of the droplets.

Figure 3.2 - Streamlines for a typical case with two droplets and $V = 1/10$.



3.3 Extinction analysis

The flamelet formulation is adopted to allow the description of the variables in the direction normal to the flame. Introducing the mixture fraction Z as an independent variable one has (PETERS, 1983; PETERS, 1984)

$$\frac{\partial}{\partial t} \rightarrow \frac{\partial}{\partial t} + \frac{\partial Z}{\partial t} \frac{\partial}{\partial Z}, \quad \nabla \rightarrow \nabla Z \frac{\partial}{\partial Z} + \nabla_{Z\perp}, \quad (3.86)$$

in which $\nabla_{Z\perp}$ is the variation in the direction normal to ∇Z , i.e., in the direction tangential to the flame. Therefore, Eq. (3.38) can be written as

$$\frac{\partial T}{\partial t} + \frac{\partial Z}{\partial t} \frac{\partial T}{\partial Z} + \mathbf{u} \cdot \left(\nabla Z \frac{\partial T}{\partial Z} + \nabla_{Z\perp} T \right) = \|\nabla Z\|^2 \frac{\partial^2 T}{\partial Z^2} + \nabla_{Z\perp}^2 T + 2\nabla Z \cdot \nabla_{Z\perp} \frac{\partial T}{\partial Z} + q\omega. \quad (3.87)$$

If the flame is infinitely thin the only relevant terms are the diffusive and the reactive and, in the flame, the equation reduces to

$$\frac{d^2 T}{dZ^2} = -q \frac{2}{\chi_f} Da y_O y_F \exp \left[\frac{T_a}{T_f} \left(1 - \frac{T_f}{T} \right) \right], \quad (3.88)$$

in which $\chi_f := 2\|\nabla Z\|_f^2$ is the scalar dissipation rate at the flame (PETERS, 1983). Similarly, the species conservation equations can be written as

$$\frac{d^2 y_O}{dZ^2} = s_Z \frac{2}{\chi_f} Da y_O y_F \exp \left[\frac{T_a}{T_f} \left(1 - \frac{T_f}{T} \right) \right], \quad (3.89)$$

$$\frac{d^2 y_F}{dZ^2} = \frac{2}{\chi_f} Da y_O y_F \exp \left[\frac{T_a}{T_f} \left(1 - \frac{T_f}{T} \right) \right]. \quad (3.90)$$

From the Large Activation Energy Asymptotics, the problem of determining the conditions of extinction of a diffusion flame can be transformed into the analysis of the existence of the solution of a boundary value problem, called canonical form (LIÑÁN, 1974). This transformation is detailed in Appendix B and, through the definition of the reduced Damköhler number δ as

$$\delta := \frac{4}{\chi_f} \frac{\varepsilon^3 s_Z Da}{q(T'^- - T'^+)} \quad (3.91)$$

and the coefficient γ as

$$\gamma := \frac{T'^+ + T'^-}{T'^+ - T'^-} \quad (3.92)$$

in which $\varepsilon := T_f^2/T_a$ and

$$T'^+ := \left. \frac{dT}{dZ} \right|_{Z=1^+}, \quad T'^- := \left. \frac{dT}{dZ} \right|_{Z=1^-}, \quad (3.93)$$

the flame is found to be extinguished if δ is smaller than a critical value δ_E , given approximately by (LIÑÁN, 1974)

$$\delta_E = e[(1 - |\gamma|) - (1 - |\gamma|)^2 + 0.26(1 - |\gamma|)^3 + 0.055(1 - |\gamma|)^4]. \quad (3.94)$$

It is relevant to point out that T'^+ is the gradient of T inside the flame (i.e., where $Z > 1$) and T'^- is the gradient of T outside the flame (where $Z < 1$).

It can be defined a critical Damköhler number Da_E such that the flame is found to be extinguished if $Da < Da_E$, with

$$Da_E := \chi_f \frac{T'^- + |T'^+|}{4} \frac{q}{\varepsilon^3 s_Z} \delta_E, \quad (3.95)$$

where it was used the fact that $T'^+ < 0$.

In the limit of small $\sqrt{\varepsilon}$ it was found that T is constant inside the flame (vid. Eq.

(3.67)), leading to $T'^+ \rightarrow 0$. Then, the magnitude of the gradient of temperature can be expected to be much larger outside of the flame than inside of it (i.e., $|T'^-| \gg |T'^+|$) and, from Eq. (3.92), $\gamma \approx -1$. Therefore, the higher order terms in Eq. (3.94) can be neglected and the critical value of δ can be approximated as $\delta_E \approx e(1 - |\gamma|)$, leading to

$$\delta_E \approx e(1 - |\gamma|) = e \left(1 + \frac{T'^- - |T'^+|}{T'^- + |T'^+|} \right) = 2e \frac{|T'^+|}{T'^- + |T'^+|}, \quad (3.96)$$

and the critical Damköhler number can be approximated as

$$Da_E = \frac{e\chi_f}{2} \frac{1}{\varepsilon^3} \frac{q}{s_Z} |T'^+|. \quad (3.97)$$

3.3.1 Estimation of the gradient of temperature inside the flame

The boundary condition for T at the droplets (Eq. (3.44)) can be written as

$$\frac{dT}{dZ} = -\frac{\sqrt{\epsilon}}{s_Z} (T - T_b + l), \quad (3.98)$$

which follows from Eq. (3.76) (which is the boundary condition for Z at the droplets) and the identity $\nabla T = \nabla Z dT/dZ$, which follows from the chain rule. In the limit of small $\sqrt{\epsilon}$ the gradient of temperature inside the flame is 0 and the temperature inside the flame is constant and equal to the temperature of the flame, i.e., T_f . For $\sqrt{\epsilon} \neq 0$, it is assumed that dT/dZ is of order $\sqrt{\epsilon}$ inside the flame and, therefore, the deviation of T from the asymptotic solution $T = T_f$ is of order $\sqrt{\epsilon}$, i.e., $T = T_f + O(\sqrt{\epsilon})$. Therefore, Eq. (3.98) can be written as

$$\frac{dT}{dZ} = -\frac{\sqrt{\epsilon}}{s_Z} (T_f - T_b + l) + O(\epsilon), \quad (3.99)$$

and T'^+ can be approximated as $T'^+ \approx -K\sqrt{\epsilon}$, with the constant K given by

$$K := \frac{T_f - T_b + l}{s_Z} = \frac{le^\beta}{s_Z}, \quad (3.100)$$

in which the relation with β follows from Eq. (3.70). The critical Damköhler number is therefore given by

$$Da_E = \frac{eK}{2} \frac{\sqrt{\epsilon}}{\varepsilon^3} \frac{q}{s_Z} \chi_f. \quad (3.101)$$

The critical Damköhler number depends only of the parameters of the problem (through K , ϵ , ε , q and s_Z) and the distribution of Z (through χ_f). Since Da_E is

proportional to χ_f , it must be evaluated at each point of the flame surface. It must be noticed that a large Da_E implies that the flame is more unstable, while a small Da_E implies that the flame is more stable. In the limit case of $Da_E = 0$, the flame cannot be extinguished.

3.4 Regarding the singularity at the droplets

For the special case of one isolated droplet, the problem reduces to

$$\frac{\partial Z}{\partial t} + \frac{1}{\tilde{r}^2} \frac{\partial}{\partial \tilde{r}} \left(\sqrt{\epsilon} \lambda Z - \tilde{r}^2 \frac{\partial Z}{\partial \tilde{r}} \right) = 0, \quad (3.102)$$

$$\tilde{r}^2 \frac{\partial Z}{\partial \tilde{r}} = -s_Z \lambda, \quad \tilde{r} \rightarrow 0, \quad (3.103)$$

$$Z = 0, \quad \tilde{r} \rightarrow \infty, \quad (3.104)$$

with \tilde{r} here representing the radial coordinate in spherical coordinates. It will be assumed that the vaporization rate is constant and given by $\lambda \equiv \beta$ (i.e., the droplet radius is constant) and that a permanent regime solution is achieved. The general solution of the governing equation for Z satisfying the boundary condition at infinity is

$$Z = C \left[1 - \exp \left(-\frac{\sqrt{\epsilon} \beta}{\tilde{r}} \right) \right]. \quad (3.105)$$

Since $dZ/d\tilde{r} = 0$ at $\tilde{r} = 0$, the boundary condition for $\tilde{r} \rightarrow 0$ cannot be applied. However, Z can be expanded in Taylor series around $\tilde{r} = \infty$ as

$$Z = C \frac{\sqrt{\epsilon} \beta}{\tilde{r}} + O \left(\frac{\epsilon \beta^2}{\tilde{r}^2} \right). \quad (3.106)$$

Therefore, if $\tilde{r} \gg \sqrt{\epsilon} \beta$, Z can be approximated as

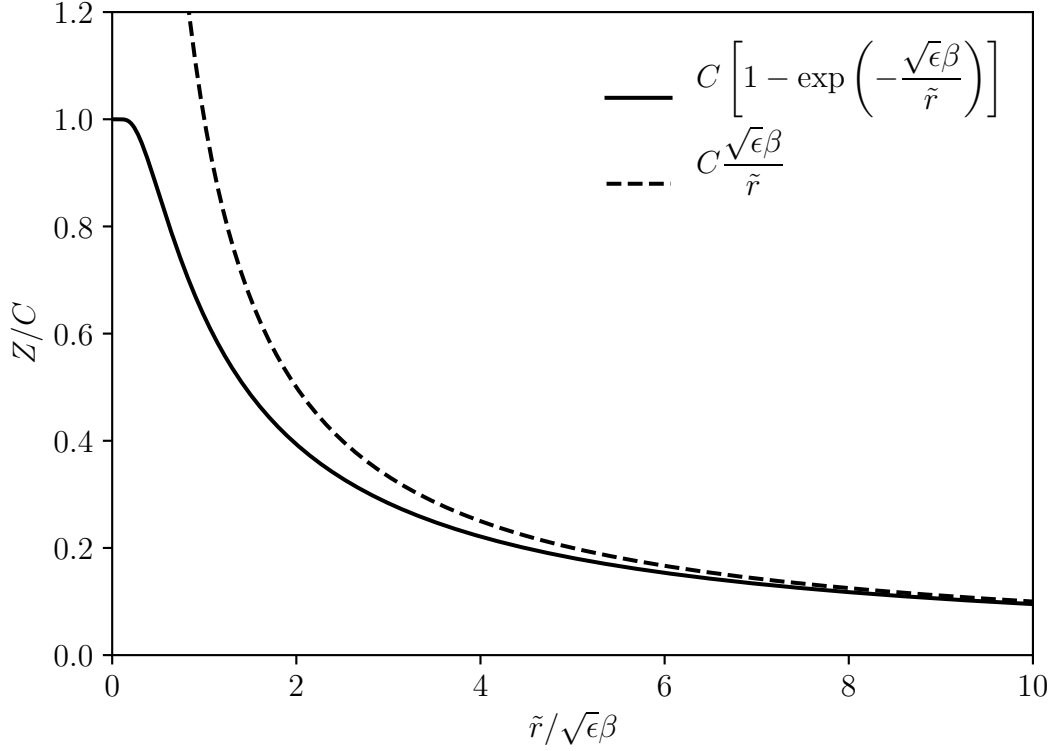
$$Z \approx C \frac{\sqrt{\epsilon} \beta}{\tilde{r}}. \quad (3.107)$$

The boundary condition at $\tilde{r} \rightarrow 0$ can now be applied, leading to $C = s_Z / \sqrt{\epsilon} = S_Z$ and

$$Z = \frac{s_Z \beta}{\tilde{r}}. \quad (3.108)$$

The asymptotic agreement between both solutions for Z is depicted in Fig. (3.3), showing that the analytical solution is incompatible with the prescribed boundary condition, although the asymptotic solution for $\tilde{r} \rightarrow \infty$ has behavior consistent with the boundary condition.

Figure 3.3 - Solution for Z in the stationary case.



Therefore, from a numerical point of view, the boundary condition for $\tilde{r} \rightarrow 0$ can be applied only at a sufficient distance to the droplet because the behavior of the boundary condition cannot be supported by the governing equation for Z much close to the droplet. Then, a ball with radius $r_{bk} \sim \sqrt{\epsilon\beta}A_k$ and center in the droplet k must be excluded from the domain, and the boundary condition

$$\tilde{r}^2 \frac{\partial Z}{\partial \tilde{r}} = -s_Z \lambda \quad (3.109)$$

must be applied in the boundary of this ball. Therefore, the boundary condition for Z for the more general case, in vectorial form, will be applied numerically as

$$\nabla Z \cdot \mathbf{e}_{Rk} = -\frac{s_Z \lambda^2}{r_{bk}^2}, \quad \|\mathbf{r} - \mathbf{r}_k\| = r_{bk}. \quad (3.110)$$

This difficulty in the application of the boundary condition at the droplets can be viewed from another point of view by noticing that Eq. (3.108) is the exact solution of the equation

$$\frac{d}{d\tilde{r}} \left(\sqrt{\epsilon\beta} Z - \frac{1}{\tilde{r}^2} \frac{dZ}{d\tilde{r}} \right) = -\frac{s_Z \sqrt{\epsilon\beta}^2}{\tilde{r}^2}, \quad (3.111)$$

which is identical to Eq. (3.102) (after the application of the considerations of permanent regime and $\lambda = \beta$) except for a source term in the right-hand side. Therefore, the application of the boundary condition Eq. (3.103) makes the equation for Z non-conservative. Also, for large \tilde{r} the source term is negligible and both equations are identical in the limit $\tilde{r} \rightarrow \infty$. Therefore, if the boundary condition at the droplets must be applied, the equation must be solved only for large \tilde{r} .

In that case, the magnitude of the gradient of Z is limited by $s_Z \lambda / r_b^2$. Defining $r_b = k\sqrt{\epsilon}\beta$, with k being a constant and recalling $\chi = 2\|\nabla Z\|^2$, the critical Damköhler number of extinction is limited by $Da_E \leq Da_{E\max}$, with

$$Da_{E\max} = \frac{eK}{(\epsilon\sqrt{\epsilon})^3} \frac{qs_Z}{(k^2\beta)^2}, \quad (3.112)$$

where it was used $\lambda/\beta = a \leq 1$.

3.5 Numerical scheme

The physical domain is approximated by a numerical domain $0 \leq r \leq L_r$, $0 \leq z \leq L_z$, in which L_r and L_z are the domain sizes in r and z directions, respectively. To properly address the boundary conditions imposed by the droplets the regions surrounding each one is removed from the domain, as explained in the previous section. The domain is discretized with a uniform rectangular mesh with resolution Δr and Δz in directions r and z , respectively, and Eq. (3.72) is discretized following the FTCS scheme, in which the spatial derivatives are substituted with centered discretizations, e.g.,

$$\frac{\partial Z}{\partial r} \approx \frac{Z_{i,j+1} - Z_{i,j-1}}{2\Delta r}, \quad (3.113)$$

in which i and j are the indexes in z and r directions, respectively. The boundary conditions for the discretized problem are: far from the droplets:

$$Z_{1,j} = Z_{N_z,j} = Z_{i,N_r} = 0, \quad (3.114)$$

in which $N_z = 1 + L_z/\Delta z$ and $N_r = 1 + L_r/\Delta r$ are the number of points in the mesh in directions z and r , respectively; at the symmetry axis:

$$Z_{i,1} = Z_{i,2}, \quad (3.115)$$

and at the contour of the region surrounding the droplets:

$$Z_{i,j} = \left(r_j \pm (z_i - z_k) \frac{\Delta r}{\Delta z} \right)^{-1} \left[\frac{s_Z \lambda_k \Delta r}{\sqrt{r_j^2 + (z_i - z_k)^2}} + r_j Z_{i,j+1} \pm (z_i - z_k) \frac{\Delta r}{\Delta z} Z_{i \pm 1, j} \right], \quad (3.116)$$

which follows from the discretization of Eq. (3.76). The time step was calculated as (HINDMARSH et al., 1984)

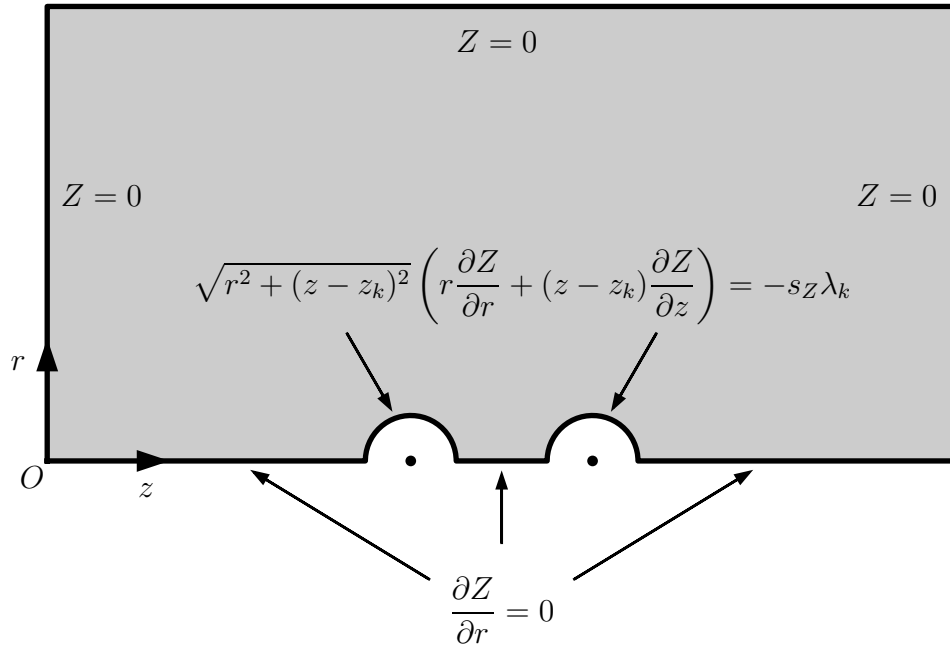
$$\Delta t \leq \min \left(\frac{(\Delta z \Delta r)^2}{2(\Delta z^2 + \Delta r^2)}, \frac{2}{U_{\max}^2} \right), \quad (3.117)$$

in which $U_{\max} = \sqrt{\epsilon}(V + \beta/r_b^2)$ is the maximum magnitude of the velocity in the domain.

The numerical domain for a case with two droplets (represented by dots) and the boundary conditions applied at each region of the boundary of the domain are shown in Fig. (3.4).

Although the regions surrounding the droplets are not part of the domain, the equation is solved in these regions, which has no effect in the solution inside the domain. Once the droplet is vaporized, the region which was surrounding it is incorporated into the domain, the boundary condition Eq. (3.116) is no longer applied and the symmetry boundary condition is applied in $r = 0$.

Figure 3.4 - Representation of the numerical domain for a case with two droplets.



4 VALIDATION

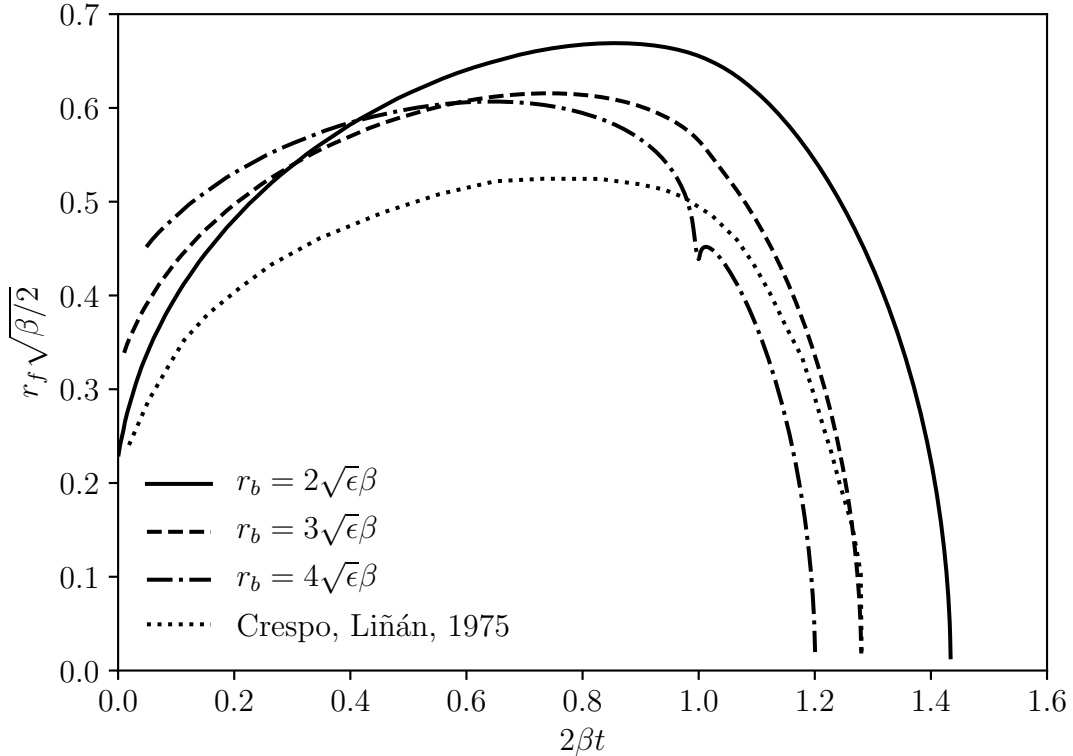
It was tried to reproduce analytical results for the flame radius (CRESPO; LIÑÁN, 1975) for the case $\alpha = 1$, in which α is a parameter relating the vaporization time of the droplet and the time in which the flame vanishes and is defined as (CRESPO; LIÑÁN, 1975)

$$\alpha := \frac{\sqrt{2\pi}}{s_Z \beta^{3/2}}, \quad (4.1)$$

using $\epsilon = 0.42 \times 10^{-3}$, $\sqrt{\epsilon} s_Z^{-1} = 0.065$ and $\beta = 3.983$. The flame radius as function of time is depicted in Fig. (4.1). Several curves are presented, as it was observed that the result is dependent on r_b , i.e., the position in which the boundary condition addressing the droplets is applied. The general behavior of the flame radius is very similar to the analytical result, despite the overestimation in the flame radius.

The value of r_b has influence on the solution, although the overall behavior does not change. A more physical behavior can be expected from the solutions with larger r_b , as explained in Section 3.4. However, the initial condition will correspond to a

Figure 4.1 - Comparison of the flame radius as function of time to an analytical solution for different sizes of the ball in which the boundary condition for the droplets is applied.

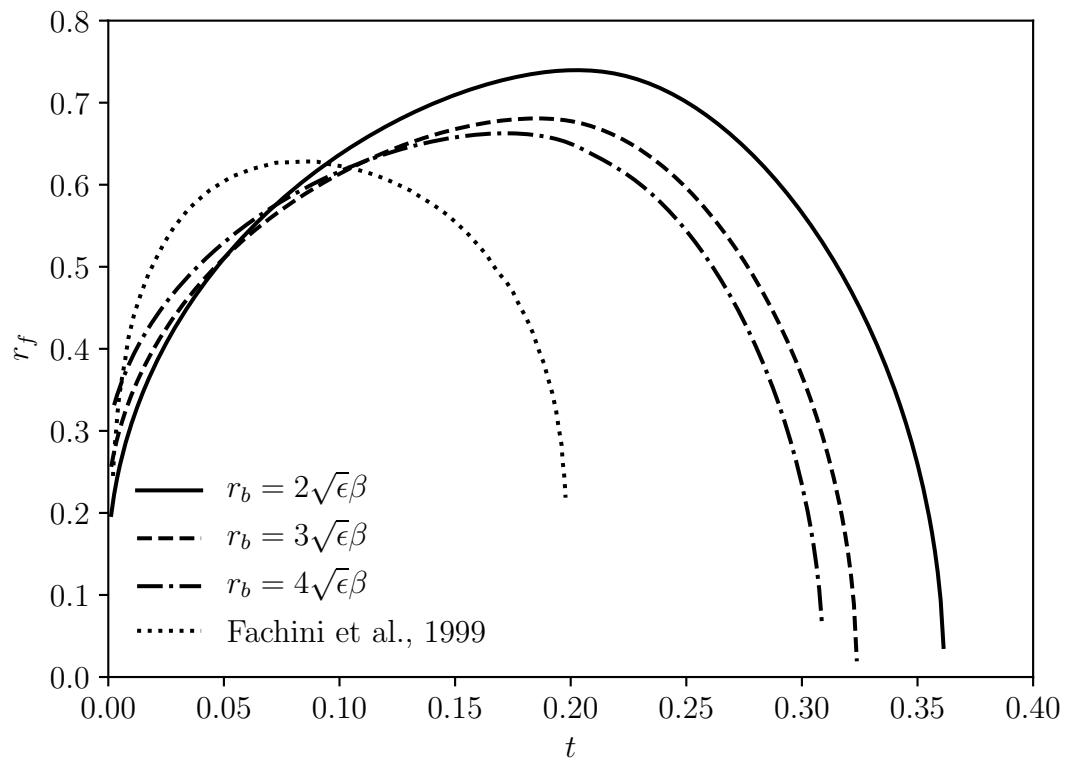


flame moving outwards with radius r_b , due to the boundary condition of imposed flux, and therefore the flame will be always larger than the analytical solution. Also, if the flame is close to the boundary of the domain in the moment that the droplet vanishes the change of the boundary condition will affect the flame, as the case $r_b = 4\sqrt{\epsilon}\beta$ shows at $2\beta t = 1$.

The fact that the solution for $r_b = 2\sqrt{\epsilon}\beta$ presents a flame much larger than the analytical solution and also a behavior different from the solutions for $r_b = 3\sqrt{\epsilon}\beta$ and $4\sqrt{\epsilon}\beta$ shows that $r_b = 2\sqrt{\epsilon}\beta$ is not sufficient for the domain to “absorb” the singularity from the boundary condition. As Fig. (3.3) shows, the singularity solution for Z has a much stronger gradient than the exact solution for small r . This stronger gradient causes a larger transport of Z close to the boundary of the domain, which is responsible by the larger flame provided by that case.

The flame radius as function of time is compared to previous results (FACHINI et al., 1999) for several r_b in Fig. (4.2). The difference between the results for the three values of r_b has the same explanation as the case presented in Fig. (4.1), with results for larger r_b presenting a larger initial flame radius and results for smaller r_b presenting larger flames due to the overestimation in the flux of Z in the boundary. Although the presented results are more consistent, they differ substantially from the results of the mentioned study due to the fact that the latter considered the effect of thermal compressibility and the transport coefficients dependence on temperature. However, the results agree in order of magnitude and the general behavior of the flame is similar.

Figure 4.2 - Comparison of the flame radius as function of time to the previous results for different sizes of the ball in which the boundary condition for the droplets is applied.



5 RESULTS

The parameters of the problem were chosen to match the ones of a previous analysis (FACHINI et al., 1999), i.e., $s_Z = 1$, $q = 5$, $T_a/T_f = 30$, $\epsilon = 10^{-3}$, $\beta = 2.534$. Also, the approximation $l = T_b$ is used for the sake of simplicity (FACHINI et al., 1999). This leads to $s_H = 0.4$, $T_f = 6$, $K = 6$, $\varepsilon = 0.2$ and $Da_E/\chi_f = 161.2$. It was used also $r_b = 3\sqrt{\epsilon}\beta = 0.24$, and the maximum Damköhler number is $Da_{E\max} = 7.1 \times 10^7$. The extinction conditions for different cases will be addressed to study the influence of the base flow and the interaction between droplets on the extinction.

5.1 Single droplet in steady ambient

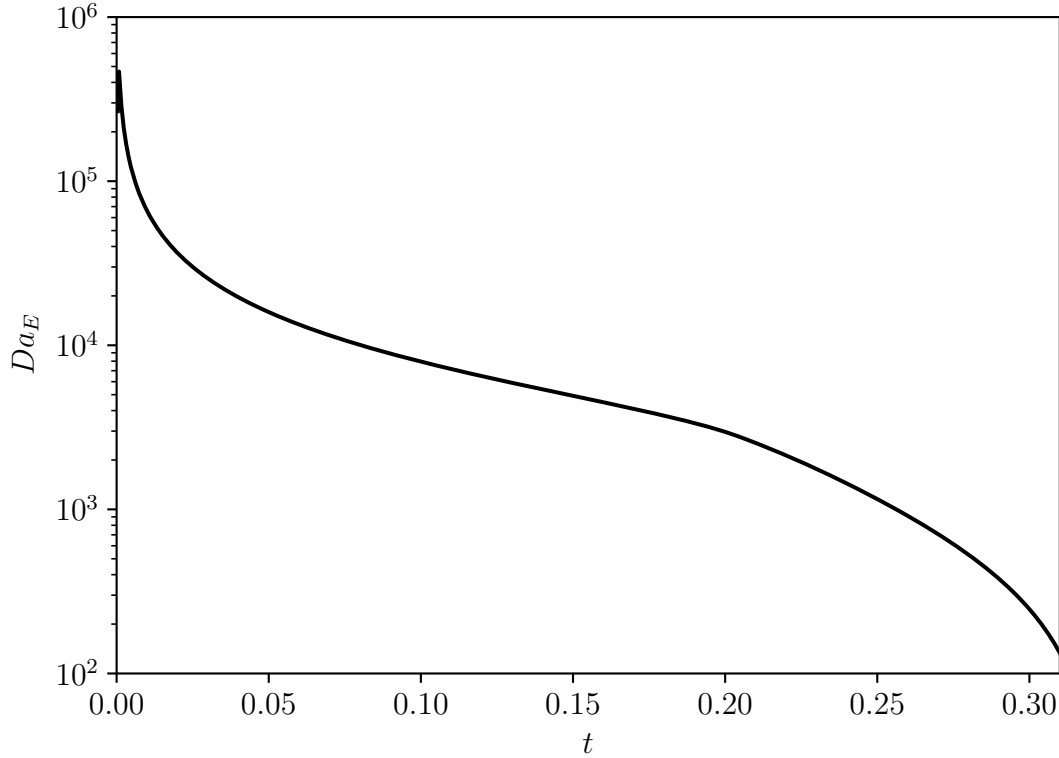
The case of the combustion of a single droplet in a steady ambient corresponds to the aforementioned problem (FACHINI et al., 1999), which also considered radiant heat loss and non-unit Lewis numbers.

The critical Damköhler number as function of time is depicted in Fig. (5.1). The droplet was completely vaporized at $t = 1/2\beta = 0.197$. It can be seen that Da_E decreases monotonically with time, and attains its maximum at $t = 0$. This is due to the fact that the flame starts at the boundary of the domain where the boundary condition for the droplet (i.e., Eq. (3.110)) is applied. Therefore, since the behavior of the flame cannot be described accurately when it is close to the boundary, the actual behavior of Da_E for small t may not be the one presented in Fig. (5.1).

The critical Damköhler number as function of the droplet radius for several values of the normalized emissivity σ was presented in the cited study (FACHINI et al., 1999), which represents the intensity of the radiant heat loss. Those results, compared to the current case, are presented in Fig. (5.2). The critical Damköhler number of the current case is larger than the critical Damköhler number for small σ and comparable to the case $\sigma = 2$, while it should be expected that the current case represents the limit $\sigma \rightarrow 0$, i.e., the case with no radiant heat loss. Therefore, Da_E for the current model should have been smaller than any of the values obtained in the mentioned study.

This unexpected behavior of Da_E can be explained by the approximations adopted in the current model, the most relevant of which is the assumption of incompressible flow (i.e., of $\rho = 1$ in the gaseous phase), while in the cited work it was considered the thermal expansion of the gaseous phase through the ideal gas law $\rho T = 1$ (FACHINI et al., 1999). It was also considered in that work the variation of the transport

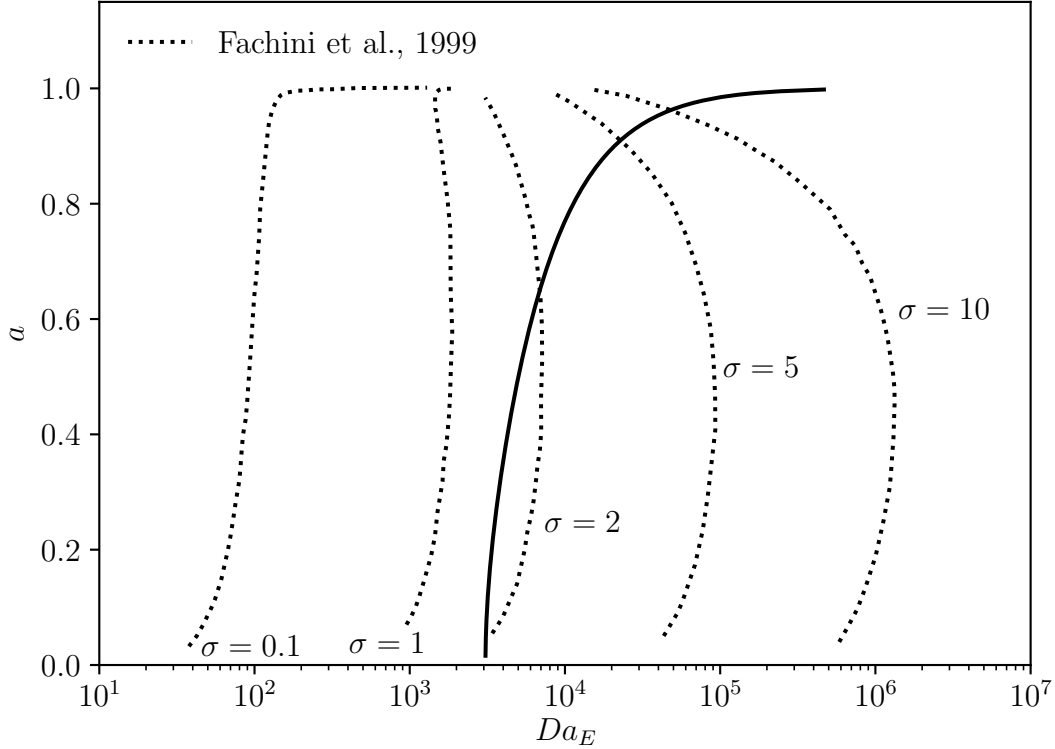
Figure 5.1 - Critical Damköhler number as function of time.



coefficients with the temperature through the relation $\rho\alpha = \sqrt{T}$ and, therefore, $1 \leq \alpha \leq 6^{3/2} = 14.70$, since the highest temperature is the flame temperature $T_f = 6$. Since the diffusivity is larger, the transport of Z could happen with a weaker gradient of Z . It must be noticed, furthermore, that the most general definition of the scalar dissipation rate is $\chi = 2\alpha\|\nabla Z\|^2$ (PETERS, 1983). Therefore, the variation of the specific mass and the transport coefficients have a direct influence in χ_f and, therefore, in the critical Damköhler number.

Another possible explanation for the difference between the results is the fact that the extinction in the current model is based solely on the heat lost by the flame to the reactants (since there is no radiant heat loss), and the heat loss to the fuel is relevant, although small (more precisely, of order $\sqrt{\epsilon}$, as derived in Section 3.3.1). If the heat loss to the fuel is not considered there cannot be extinction due solely to convective-diffusive effects, since in that case the critical Damköhler number would be $Da_E = 0$ (since Eqs. (3.92) and (3.94) would lead to $\gamma = -1$ and $\delta_E = 0$, respectively). However, the influence of order $\sqrt{\epsilon}$ in the gradient of temperature in the fuel region was neglected in the mentioned work (which can be seen comparing Eq. (31) of the cited work to Eqs. (3.61) and (3.62)), and the gradient of temperature

Figure 5.2 - Comparison of the critical Damköhler number to the cases with radiant heat loss. The line continuous represents the result of the current model and the dotted lines represent the results obtained in a previous work.



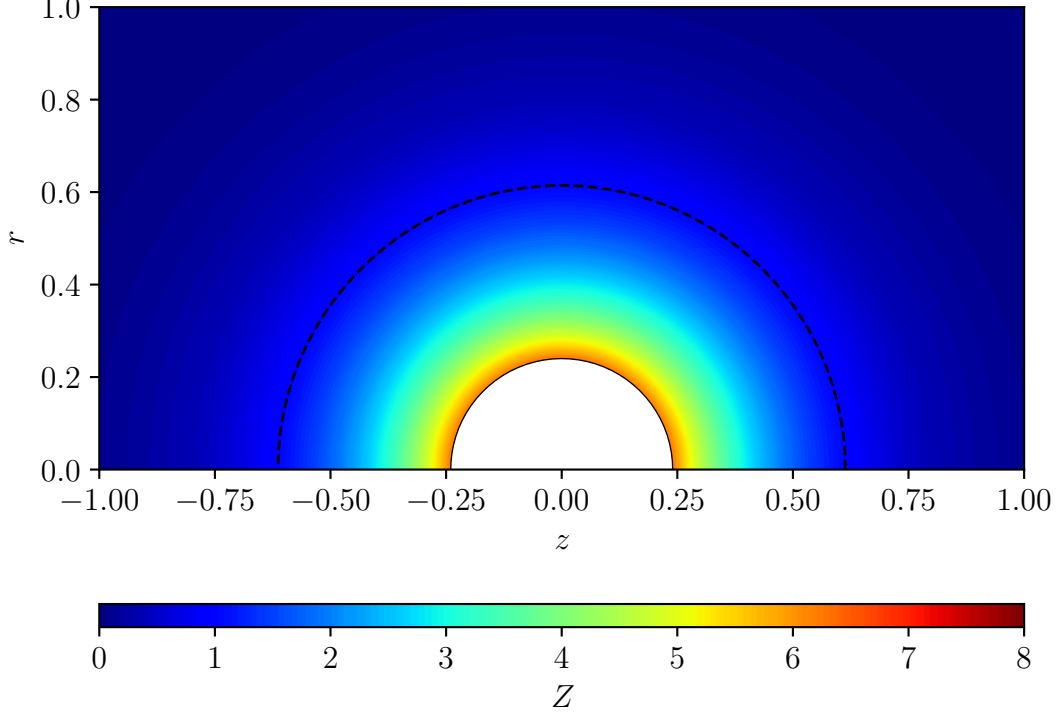
in the fuel region is not 0 only if there is radiant heat loss (FACHINI et al., 1999).

Although the results disagree in order of magnitude, the general behavior of the critical Damköhler number for the current model is similar to the behavior for $\sigma = 0.1$, which has also a monotonic dependence of time. This is due to the fact that for larger σ (i.e., for more intense radiant heat loss) the heat loss is more dependent on the flame radius, since a larger flame will lose more heat due to its larger area. For small σ , though, this dependence on the flame radius is weak, while in the absence of radiant heat loss there is no heat loss related to the flame size.

5.2 Single droplet under forced convection

The distribution of Z for the cases without forced convection (i.e., the case studied in the previous section) and the case with forced convection with velocity $V = 100$ at $t = 1/4\beta = 0.0986$, i.e., at half the vaporization time, are shown in Figs. (5.3) and (5.4), respectively. It can be seen that the overall flame size is approximately the same, but the forced convection dislocates the flame to the direction of positive

Figure 5.3 - Distribution of Z for the case without forced convection ($V = 0$) at half the vaporization time ($t = 1/4\beta = 0.0986$). The dashed line represents the flame and the white half circle is the region around the droplet excluded from the domain.



z . Therefore, the flame upstream of the droplet gets closer to it, while the flame downstream of the droplet gets farther. As a consequence, the flame upstream of the droplet has a stronger gradient of Z and, since the critical Damköhler number is proportional to $\chi_f = 2\|\nabla Z\|_f^2$, it is larger at the upstream region of the flame, that is where the flame extinguishes first. It is depicted in Fig. (5.5), which shows the critical Damköhler number along the flame.

Figure (5.6) shows the information of Fig. (5.5) parameterized by the angle θ , measured from the axis z to the line joining the center of the droplet to the position of the flame in the counterclockwise direction. It can be seen that the critical Damköhler number is larger where the flame is closer to the droplet and smaller where the flame is farther from the droplet. Also, the largest Damköhler number in that case is larger than the Damköhler number for the case without convection, which is $Da_E = 8.05 \times 10^3$, while the smallest Damköhler number is also smaller than the Damköhler number for the case without convection. As Fig. (5.7) shows, this behavior occurs for all t , and increases with time, since the effect of the convection

Figure 5.4 - Distribution of Z for the case with convection ($V = 100$) at half the vaporization time ($t = 1/4\beta = 0.0986$).

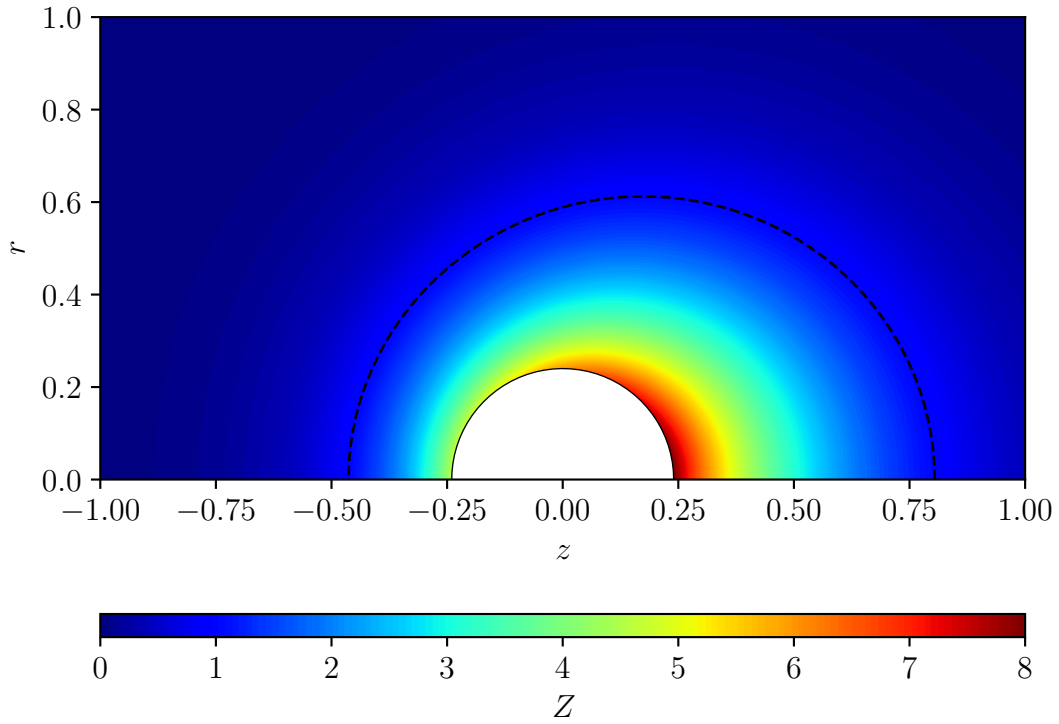


Figure 5.5 - Critical Damköhler number of extinction along the flame for the case $V = 100$ at half the vaporization time ($t = 1/4\beta = 0.0986$).

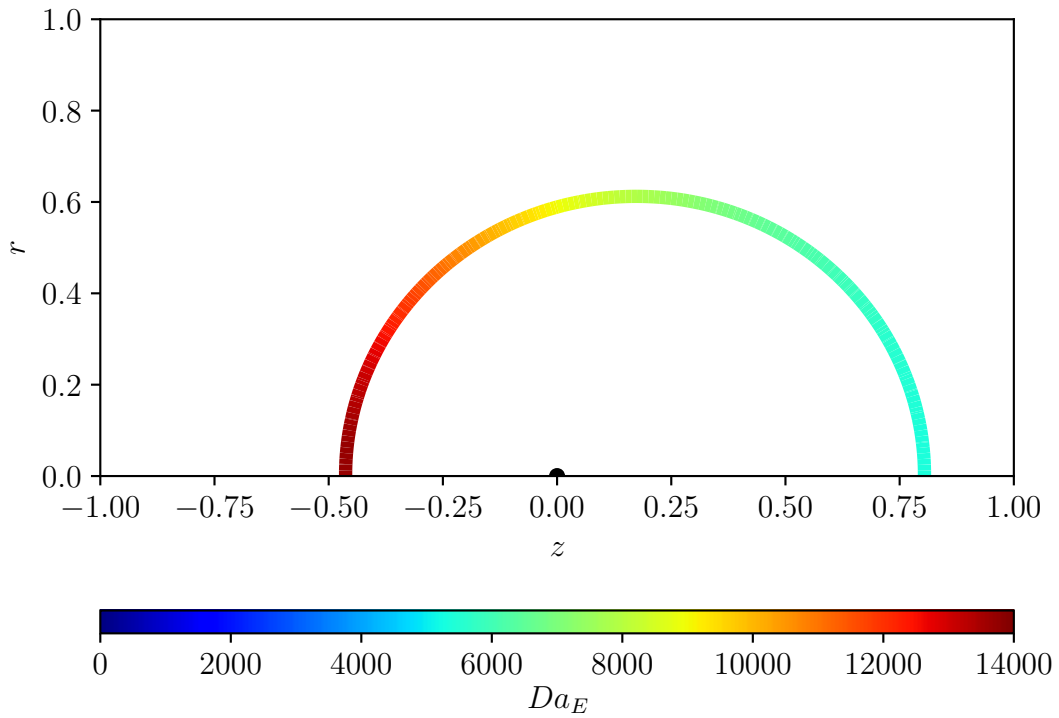
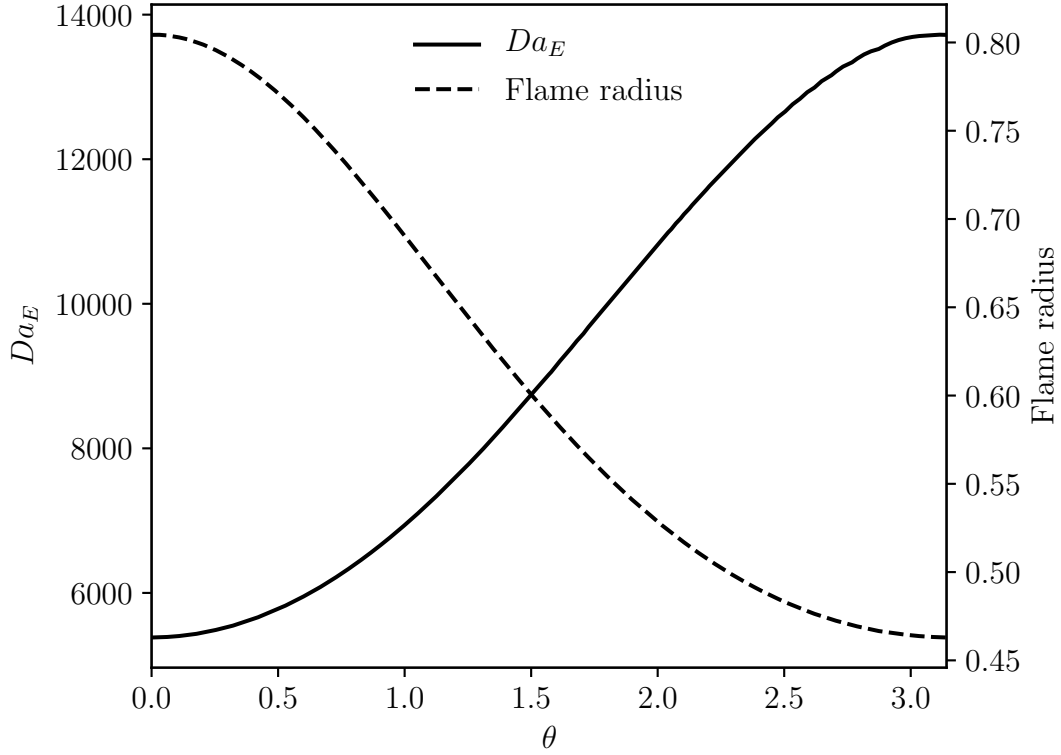


Figure 5.6 - Critical Damköhler number of extinction and flame radius as functions of the angle θ for the case $V = 100$ at half the vaporization time ($t = 1/4\beta = 0.0986$).



on the flame shape also increases with time. However, for small t and when the flame is close to vanishing the critical Damköhler number behaves in a similar fashion for all V , since the flame is closer to the droplet.

5.3 Pair of identical droplets in steady ambient

Figures (5.8) and (5.9) show the critical Damköhler number along the flame in the moment that the flames surrounding the droplets merge into one, which happens at $t = 0.0262$ and $t = 0.1012$ for identical droplets apart by a distance of 1 and 1.5, respectively. It can be seen that the smallest critical Damköhler number is at the region of merging, while the largest Damköhler number is at the extremities of the flame.

As shown in Fig. (5.10), the gradient of Z is weaker in the region between the droplets, as this region is well provided of fuel. Furthermore, at the moment of merging, the gradient of Z in the flame in the region between droplets is identically zero, since the gradient in direction r is zero (due to the axisymmetry boundary condition at $r = 0$) and the gradient in direction z is also zero, since in the moment

Figure 5.7 - Maximum critical Damköhler number as function of time for different values of V .

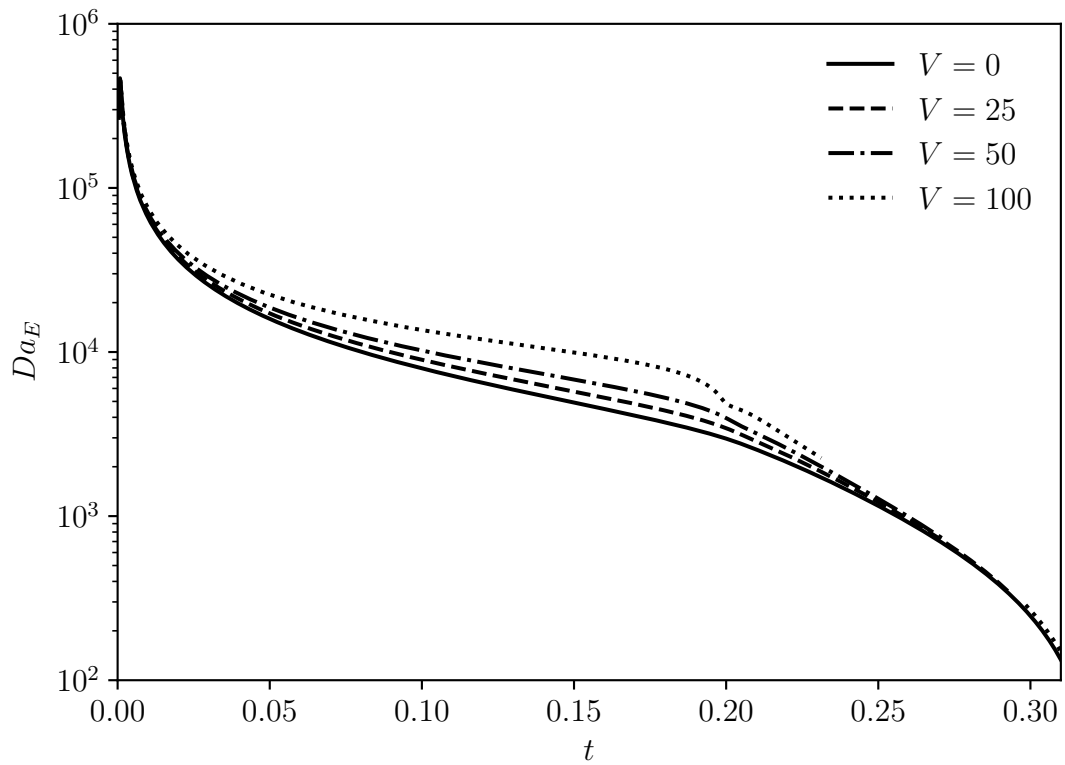


Figure 5.8 - Critical Damköhler number along the flame in the moment of merging ($t = 0.0262$) for identical droplets at distance 1.

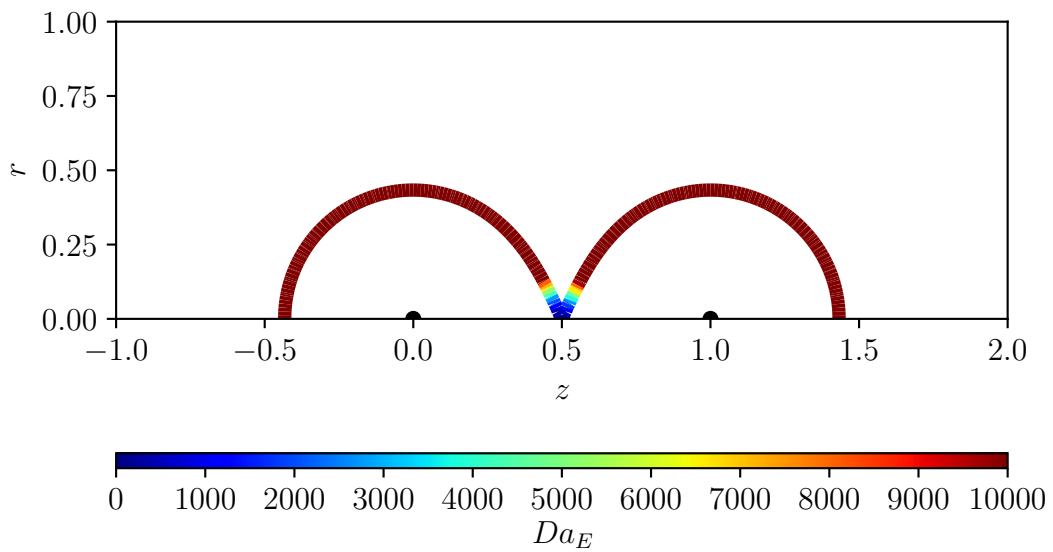


Figure 5.9 - Critical Damköhler number along the flame in the moment of merging ($t = 0.1012$) for identical droplets at distance 1.5.

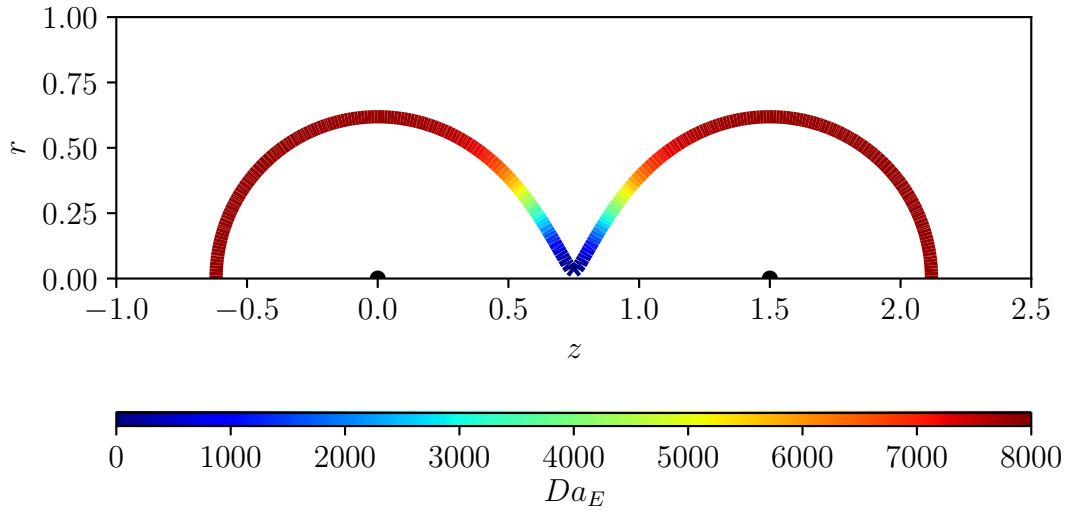
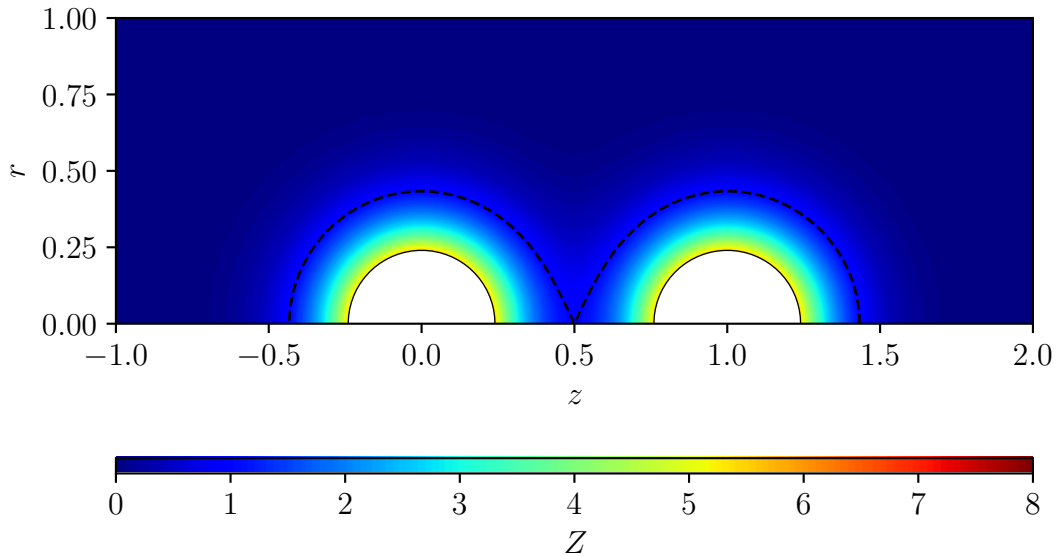
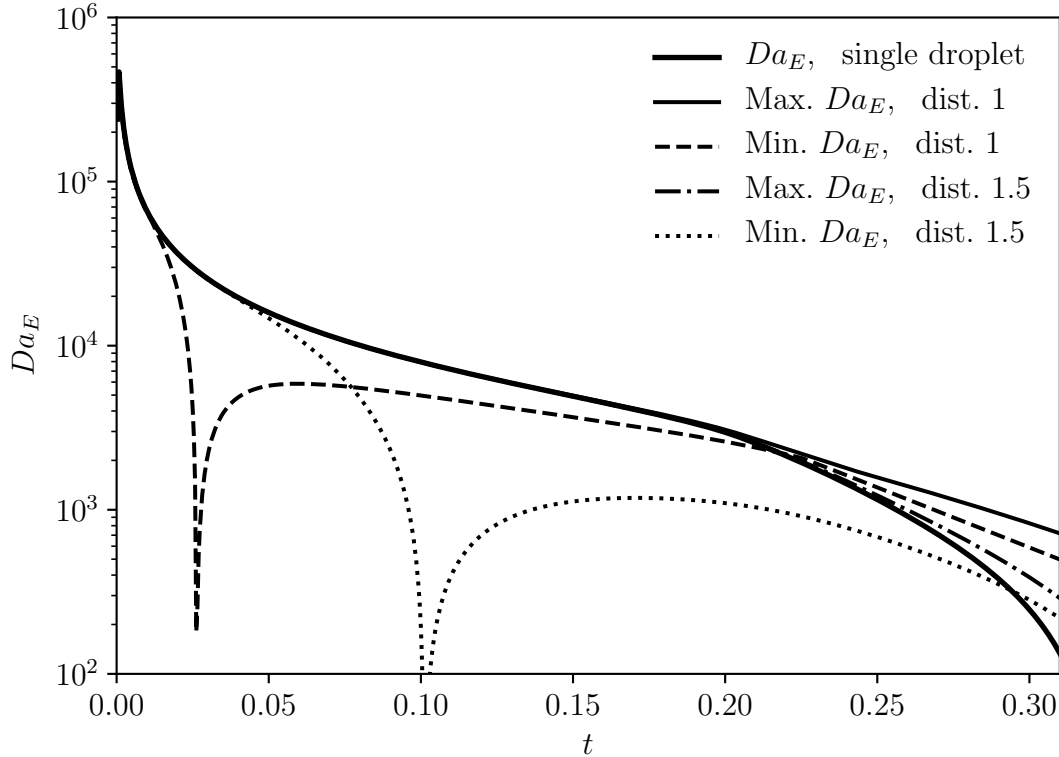


Figure 5.10 - Distribution of Z in the moment of merging for identical droplets at distance 1.



of merging between the droplets the flame is parallel to the axis z and Z is constant along the flame. Therefore, since $\|\nabla Z\| = 0$ in this region of the flame, $Da_E = 0$ in the flame between the droplets in the moment of merging, and the flame cannot be extinguished in this region. Also, since the largest Da_E is always in the extremities of the flame, the extinction will always occur in the extremities.

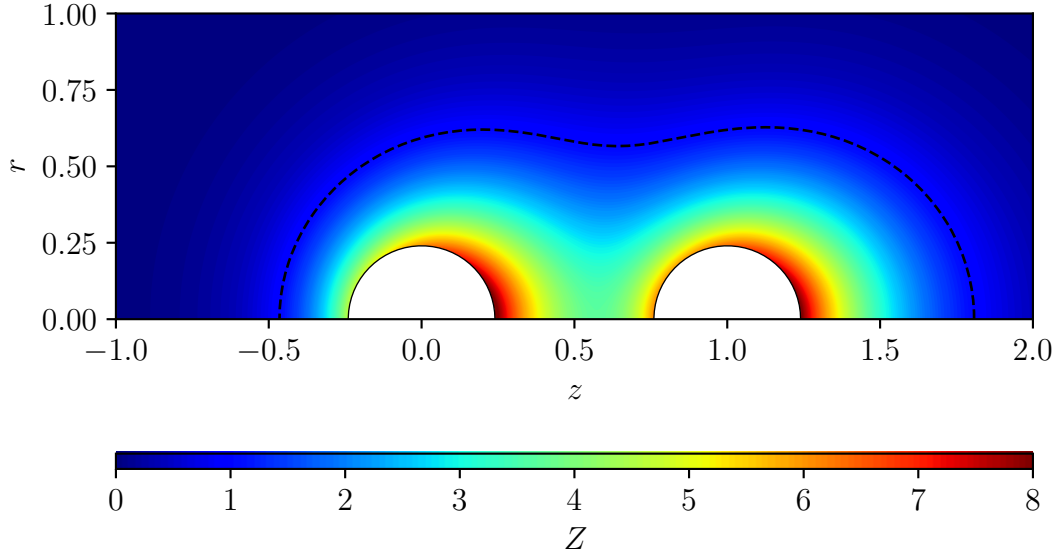
Figure 5.11 - Critical Damköhler number as function of time for the cases of a single droplet and of two identical droplets.



A more complete description of the effect of the interaction between droplets on the critical Damköhler number is depicted in Fig. (5.11). It can be seen that the maximum Damköhler number for each case (which is at the extremities of the flame) is identical to the Damköhler number for a single droplet during the droplet vaporization. After the droplet is completely vaporized, the flame vanishes slower if the droplets are close to each other, due to the larger amount of vaporized fuel left inside the flame, and the critical Damköhler number decreases slowly. The minimum Damköhler number, which is at the flame in the region between the droplets, is close to the critical Damköhler number for a single droplet for small t until the flame is affected by the other droplet, and the weaker gradient of Z makes the Damköhler number in that region decrease until it vanishes to 0 when the flames merge.

As shown in Fig. (5.11), the interaction between droplets has no effect on the extinction, since the critical Damköhler number attains its maximum at the extremities of the flame. The only effect of the interaction between droplets should be expected if the flame were to be extinguished after the droplets vaporize. Since the maximum Damköhler number decreases monotonically, the extinction can always be expected

Figure 5.12 - Distribution of Z at half the vaporization time ($t = 1/4\beta = 0.0986$) with $V = 100$ and identical droplets at distance 1.



to occur before the complete vaporization of the droplets.

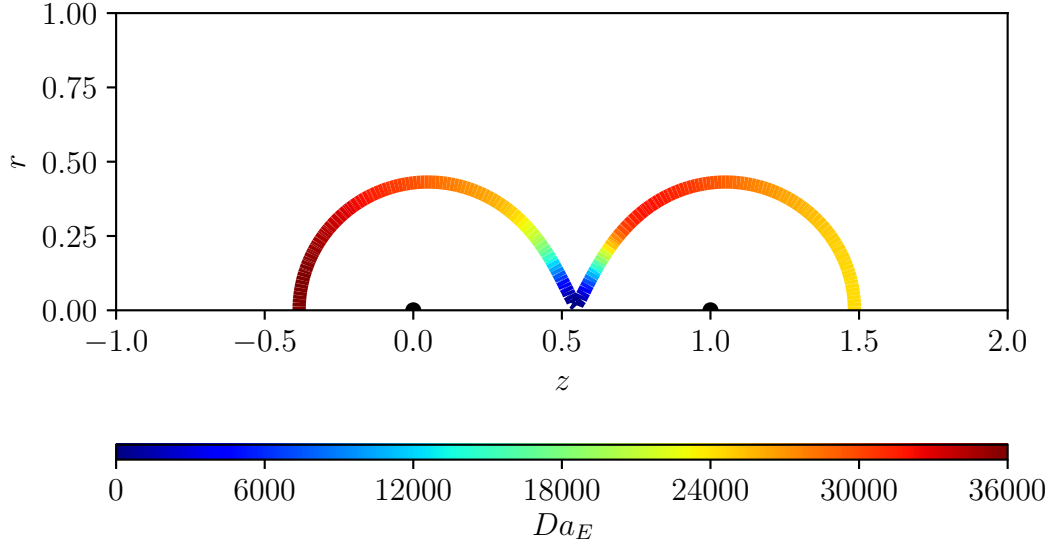
5.4 Pair of identical droplets under forced convection

Figure (5.12) shows the distribution of Z at half the vaporization time for the case of two identical droplets at distance 1 and forced convection with $V = 100$. This result is similar to the presented in Fig. (5.4) for the case of a single droplet. More specifically, the distribution of Z in the region upstream of the leftmost droplet and in the region downstream of the rightmost droplet are similar, since those regions are unaffected by the other droplet.

Figures (5.13) and (5.14) show the critical Damköhler number along the flame at the moment of merging and at half the droplets vaporization time, respectively. Similarly to the results obtained for the case of a single droplet with forced convection, the largest Damköhler number is in the flame at the upstream region and, in agreement with the results for the case of two identical droplets without forced convection, the Damköhler number in the region between droplets is small.

The behavior of the maximum Damköhler number along time is not influenced by the interaction between droplets until the droplets are completely vaporized, as it was verified for the case with no forced convection. Therefore, the behavior of the Damköhler number for $t < 1/2\beta$ (i.e., before the vaporization) is identical to the

Figure 5.13 - Critical Damköhler number along the flame in the moment of merging ($t = 0.0258$) with $V = 100$ and identical droplets at distance 1.



depicted in Fig. (5.7).

5.5 Pair of different droplets in steady ambient

Similarly to the results presented in the previous sections, it was observed no influence of the presence of a smaller droplet on the extinction. As discussed before, the gradient of Z , which value in the flame is relevant to the extinction, is limited by the value of ∇Z in the boundary of the domain (where the boundary condition addressing the droplets is applied). However, since $\|\nabla Z\| \propto \lambda = \beta a$ (vid. Eqs. (3.76) and (3.27)), the critical Damköhler number in the flame around the smaller droplet will be always smaller than the critical Damköhler number in the flame around the larger droplet. For illustration purposes, Fig. (5.15) shows the critical Damköhler number along the flame for the case with a droplet 1 at $z = 0$ with initial nondimensional radius $a_{01} = 1$ and a droplet 2 at $z = 1$ with initial nondimensional radius $a_{02} = 1/2$ at the instant of complete vaporization of the smaller droplet (i.e., at $t = a_{02}^2/2\beta = 0.050$).

5.6 Pair of different droplets under forced convection

As observed for the case of identical droplets under forced convection, the addition of a smaller droplet downstream of the first droplet has no effect on the extinction, since it will happen in the flame in the upstream region of the larger droplet, as

Figure 5.14 - Critical Damköhler number along the flame at half the vaporization time ($t = 1/4\beta = 0.0986$) with $V = 100$ and identical droplets at distance 1.

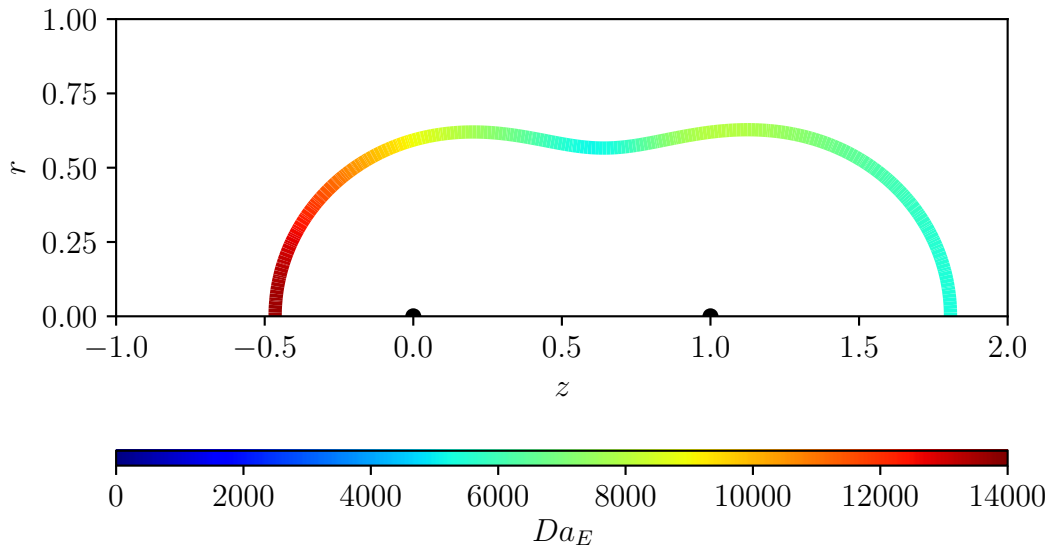


Figure 5.15 - Critical Damköhler number of extinction along the flame for two droplets with initial nondimensional radius $a_{01} = 1$ and $a_{02} = 1/2$ at the instant of complete vaporization of the smaller droplet ($t = a_{02}^2/2\beta = 0.050$).

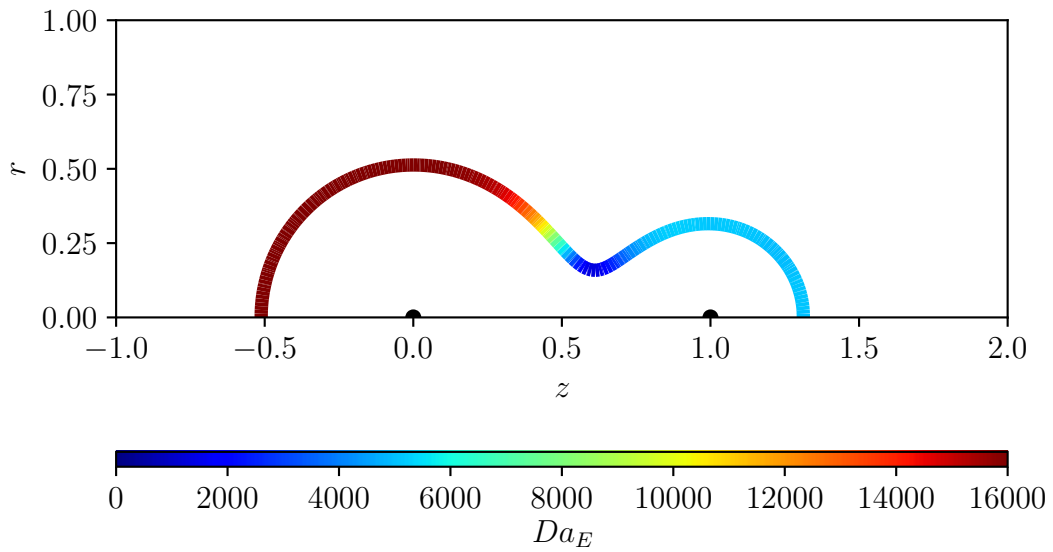
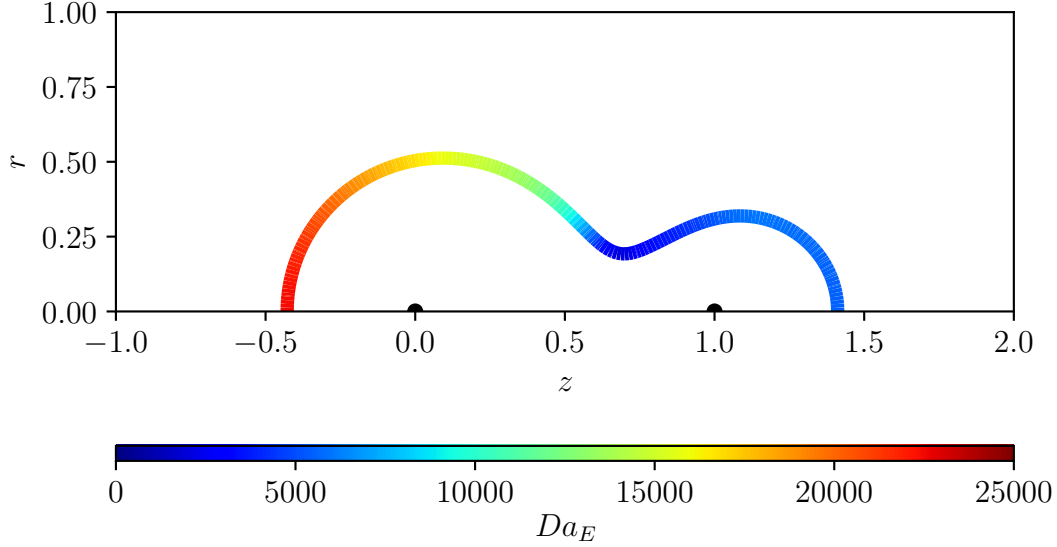


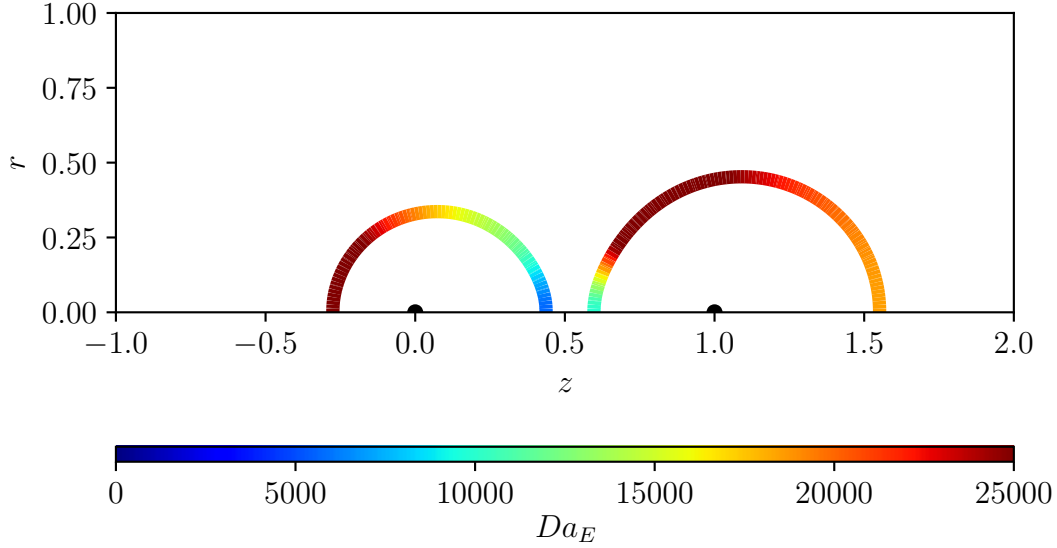
Figure 5.16 - Critical Damköhler number of extinction along the flame for two droplets with initial nondimensional radius $a_{01} = 1$ and $a_{02} = 1/2$ at the instant of complete vaporization of the smaller droplet ($t = a_{02}^2/2\beta = 0.050$) for $V = 100$.



suggested by Fig. (5.16), which shows the critical Damköhler number along the flame for the case of two droplets with initial radius $a_{01} = 1$ and $a_{02} = 1/2$ at the instant of complete vaporization of the smaller droplet ($t = a_{02}^2/2\beta = 0.050$) and with forced convection with $V = 100$.

If the smaller droplet is upstream of the larger droplet the largest critical Damköhler number will not necessarily be at the flame around the largest droplet, as it was in the cases studied in the previous sections. Figure (5.17) shows the critical Damköhler number along the flame for a case with two droplets with nondimensional initial radius $a_{01} = 1/2$ and $a_{02} = 1$, i.e., with the smaller droplet upstream of the larger droplet, and with $V = 150$. It can be seen that the highest values of Da_E occurs in two different regions, viz., the flame in the upstream region of the smaller droplet and in the flame the around the largest droplet. In the former, the large Da_E is a consequence of the flame being closer to the droplet due to the forced convection and, in the latter, because the largest droplet has also a stronger gradient of Z around it, due to its larger vaporization rate. Therefore there are two competing causes for a large critical Damköhler number. In the absence of forced convection, the largest Damköhler number will always be in the flame around the largest droplet, as stated in the previous section. However, if the forced convection is strong enough and the smaller droplet is upstream of the largest droplet, the flame in the upstream region

Figure 5.17 - Critical Damköhler number of extinction along the flame for two droplets with initial nondimensional radius $a_{01} = 1/2$ and $a_{02} = 1$ at $t = 0.031$ for $V = 150$.

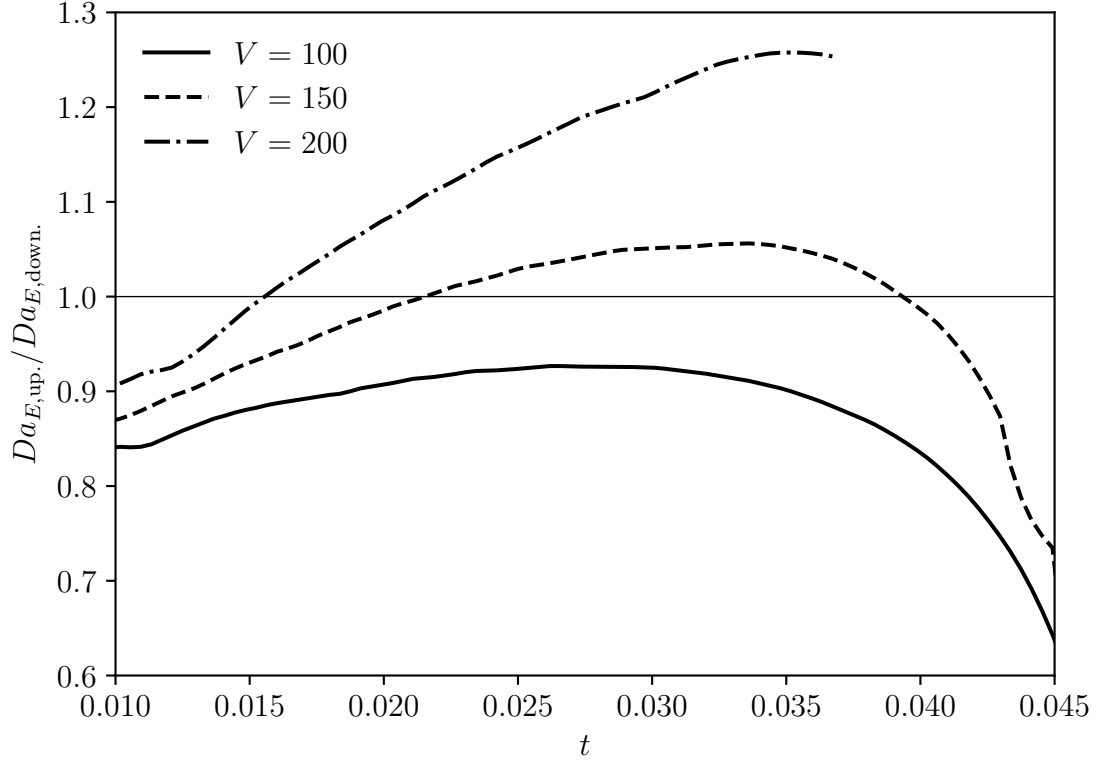


of the smaller droplet will approach it, being in a region of stronger gradient of Z than the flame around the largest droplet.

The ratio between the largest critical Damköhler number in the upstream region of the smallest droplet ($Da_{E,\text{up.}}$) and the largest critical Damköhler number in the remaining of the domain (i.e., for $z > 0$, $Da_{E,\text{down.}}$) as a function of time for different values of V is presented in Figs. (5.18) and (5.19) for smaller droplets with initial nondimensional radius $a_{01} = 1/2$ and $a_{01} = 3/4$, respectively. In all presented cases the ratio increases until reaching its maximum and then decreases to zero when the flame around the smallest droplet disappears. The curve for $V = 200$ in Fig. (5.18) is truncated due to the fact that the flame in the upstream region reached the boundary of the domain where the boundary condition for the smaller droplet is applied due to the strong forced convection.

For both cases of $a_{01} = 1/2$ and $a_{02} = 3/4$ the ratio is smaller than 1 for small t due to the fact that the effect of the forced convection on the flame increases with time, since the gradient of Z is stronger for small t (and, therefore, the diffusion was more important) and also the convection resulting from the vaporization of the droplets. Therefore, for small t the problem is similar to the case without convection and the Damköhler number in the flame around the largest droplet is larger. As t increases, the flame around the largest droplet increases in size, getting farther from

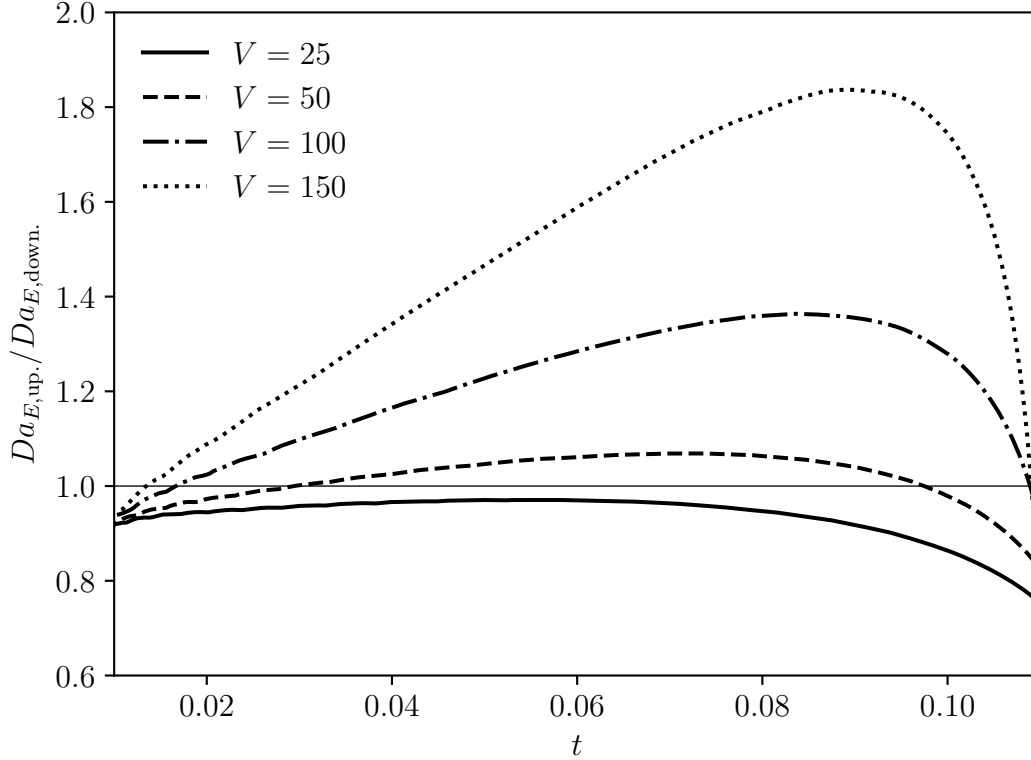
Figure 5.18 - Ratio between the critical Damköhler number at the flame in the upstream region of the smaller droplet and in the downstream region (i.e., in the remaining of the domain) as a function of t for different V for the case of two droplets with initial nondimensional radius $a_{01} = 1/2$ and $a_{02} = 1$.



the droplet and, therefore, being in a region of weaker gradient of Z (which leads to a smaller Da_E) but the flame in the upstream region of the smaller droplet does not get much far from the droplet, due to the effect of the forced convection, being in a region of stronger gradient of Z (which leads to a larger Da_E). Eventually the Damköhler number in the upstream region of the smaller droplet will be larger than the Damköhler number around the larger droplet, which is represented in the Figs. (5.18) and (5.19) when the ratio is larger than 1. As time increases, the vaporization of the smaller droplet gets weaker and so does the gradient of Z . Therefore, the critical Damköhler number in the upstream region starts to decrease until the smaller droplet vaporizes completely, and the ratio goes to 0.

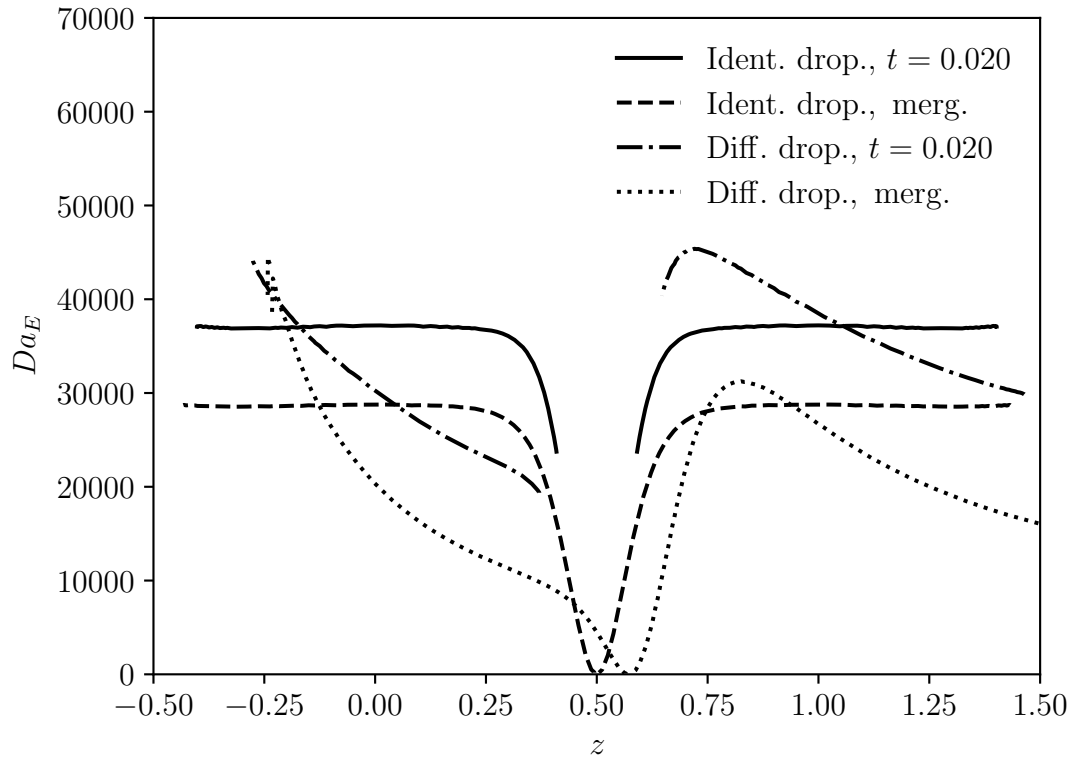
Figure (5.20) shows the distribution of the critical Damköhler number along the flame for the case of equal droplets in steady ambient (studied in Section 5.3) and of different droplets under forced convection with $V = 150$ (as in Fig. (5.17)). The depicted curves correspond to $t = 0.020$ and to the instant of merging for each case,

Figure 5.19 - Ratio between the critical Damköhler number at the flame in the upstream region of the smaller droplet and in the downstream region (i.e., in the remaining of the domain) as a function of t for different V for the case of two droplets with initial nondimensional radius $a_{01} = 3/4$ and $a_{02} = 1$.



which is at $t = 0.0258$ for the case of identical droplets and at $t = 0.0430$ for the case of different droplets. The monotonic behavior of the Damköhler number from the extremity of the flame to the flame in the region between the droplets is shown for the case of identical droplets, but the behavior of the Damköhler number for the case of different droplets is not so simple, especially in the flame around the larger droplet (i.e., in the rightmost part of the curves). In particular, the behavior of the Damköhler number along the flame around the larger droplet is not monotonic, since the upstream region of the larger droplet is the closer to the other droplet and, although the flame is closer to the larger droplet in that region (which should increase the gradient of Z in the flame), the flame is in a region of weaker gradient of Z . The Damköhler number in the flame in the downstream region of the larger droplet is small because the flame is far from the droplet and, therefore, in a region of weak gradient of Z . Simultaneously, in the flame in the upstream region of the larger droplet is also in a region of weak gradient of Z , due to the smaller droplet which also provides fuel to that region. Therefore, since there are two points in the

Figure 5.20 - Comparison between the distribution of the critical Damköhler number along the flame for the case of identical droplets in steady ambient and the case of different droplets (with initial nondimensional radius $a_{01} = 1/2$ and $a_{02} = 1$) under forced convection with $V = 150$ at $t = 0.020$ and at the instant of merging.



flame in opposite regions of the droplet with small Damköhler number, the maximum Damköhler number in the flame around the larger droplet cannot be somewhere in $r = 0$, as it is with the smaller droplet or in the other studied cases, but somewhere else in the upstream region of the larger droplet, which is also show in Fig. (5.17).

6 CONCLUSIONS

In this work a simplified model for droplet combustion was developed to investigate the extinction conditions for the diffusion flame around droplets. After the introduction of the Zeldovich and flamelet formulations, an expression was found for the critical Damköhler number of extinction (Eq. (3.101)), proportional to the scalar dissipation rate at the flame $\chi_f = 2\|\nabla Z\|^2$ and, therefore, the extinction could be availed after the solution of the governing equation for Z for any configuration of droplets and external flow. Although the problem was solved only for the axisymmetric case of droplets placed over a straight line, the vectorial formulation of the Eqs. (3.56) to (3.61) allows for the description of any configuration of droplets in two dimensions.

The behavior of the critical Damköhler number for a case of a single droplet in a steady ambient (i.e., without forced convection) was found to be the archetypal of the extinction for the several presented cases, although a comparison to results of previous works revealed differences that could not be totally explained (FACHINI et al., 1999). It was found that the critical Damköhler number decreases with time, which implies that the flame gets more stable while the droplet vaporizes and, after the complete vaporization of the droplet, while the flame reigrdes. Since the Damköhler number decreases monotonically, the flame will not be extinguished if it was ignited in the first place, unless some other phenomena cause a change in the Damköhler number (a sudden change in the droplet configurations, for example). However, since the model cannot describe the flame in the inner zone, the distribution of Z is not described well by the model for small t and, therefore, the behavior of the Damköhler number may be different from the presented for small t .

It was found that the presence of forced convection increases the critical Damköhler number, and the effect of the forced convection over the Damköhler number increases with time until the vaporization of the droplet, and its effect starts vanishing. Therefore, for small t and close to the vanishing of flame the behavior of the Damköhler number is the same for any intensity of forced convection.

For the case of interacting droplets it was found that the largest Damköhler number is always in the flame around the largest droplet in the region unaffected by the other droplet, while the smallest Damköhler number is in the flame between the droplets, meaning that the flame between the droplets is the most stable. Since the largest Damköhler number is unaffected by the smaller droplet, the extinction of a single droplet occurs in the same condition for the same single droplet accompanied by

another droplet of the same size or smaller, i.e., the extinction of the flame around a droplet is not affected by the addition of another droplet. The same was observed for the cases with forced convection, unless a smaller droplet is placed in the upstream region of the largest droplet, in which case the largest Damköhler number can be found around the smaller droplet if the convection is strong enough.

6.1 Future work

Some of the considerations that were adopted, such as constant transport coefficients and unitary Lewis numbers, could be suppressed without further difficulties in an eventual expansion of the model. The most important considerations, however, are the assumption of potential flow and the assumption that the flame is always in the transient region. While the model could be easily adapted so that the flow is determined by the Navier-Stokes equations, the modelling of the flame in the quasisteady region would require further developments, if not a whole new model.

REFERENCES

- ALMAGRO, A.; FLORES, O.; VERA, M.; LIÑÁN, A.; SÁNCHEZ, A. L.; WILLIAMS, F. A. Effects of differential diffusion on nonpremixed-flame temperature. **Proceedings of the Combustion Institute**, 2018. 16
- ANNAMALAI, K.; RYAN, W. Interactive processes in gasification and combustion. part i: liquid drop arrays and clouds. **Progress in Energy and Combustion Science**, v. 18, n. 3, p. 221–295, 1992. 4
- BRZUSTOWSKI, T. A.; TWARDUS, E. M.; WOJCICKI, S.; SOBIESIAK, A. Interaction of two burning fuel droplets of arbitrary size. **AIAA Journal**, v. 17, n. 11, p. 1234–1242, 1979. 4
- CALDEIRA, A. B.; FACHINI, F. F. Nonunitary lewis number effects on the combustion of a linear array of gaseous fuel pockets. **Numerical Heat Transfer**, v. 58, n. 10, p. 784–801, 2010. 6
- CHEATHAM, S.; MATALON, M. A general asymptotic theory of diffusion flames with application to cellular instability. **Journal of Fluid Mechanics**, v. 414, p. 105–144, 2000. 16
- CHIANG, C.; RAJU, M.; SIRIGNANO, W. Numerical analysis of convecting, vaporizing fuel droplet with variable properties. **International Journal of Heat and Mass Transfer**, v. 35, n. 5, p. 1307–1324, 1992. 5
- CHIGIER, N.; MCCREATH, C. Combustion of droplets in sprays. **Acta Astronautica**, v. 1, n. 5-6, p. 687–710, 1974. 4
- CRESPO, A.; LIÑÁN, A. Unsteady effects in droplet evaporation and combustion. **Combustion Science and Technology**, v. 11, n. 1-2, p. 9–18, 1975. 5, 8, 9, 13, 29
- FACHINI, F.; LIÑÁN, A.; WILLIAMS, F. A. Theory of flame histories in droplet combustion at small stoichiometric fuel–air ratios. **AIAA**, v. 37, p. 1426–1435, 1999. 3, 13, 15, 17, 30, 33, 35, 51
- FACHINI, F. F. The effects of the acoustic field on droplet extinction processes. **Combustion Science and Technology**, v. 120, n. 1-6, p. 237–253, 1996. 3
- _____. Transient effects in the droplet combustion process in an acoustically perturbed high temperature environment. **Combustion Science and Technology**, v. 139, n. 1, p. 173–189, 1998. 3

- _____. An analytical solution for the quasi-steady droplet combustion. **Combustion and Flame**, v. 116, n. 1, p. 302–306, 1999. 3
- FACHINI, F. F.; LIÑÁN, A. Transient effects in droplet ignition phenomenon. **Combustion and Flame**, v. 109, n. 3, p. 303–313, 1997. 3
- FAETH, G. M. Current status of droplet and liquid combustion. **Progress in Energy and Combustion Science**, n. 3, p. 191–224, 1977. 4
- _____. Evaporation and combustion of sprays. **Progress in Energy and Combustion Science**, v. 9, n. 1-2, p. 1–76, 1983. 4
- FRANZELLI, B.; VIÉ, A.; IHME, M. On the generalisation of the mixture fraction to a monotonic mixing-describing variable for the flamelet formulation of spray flames. **Combustion Theory and Modelling**, v. 19, n. 6, p. 773–806, 2015. 6
- GODSAVE, G. A. E. Studies of the combustion of drops in a fuel spray—the burning of single drops of fuel. **Symposium (International) on Combustion**, v. 4, n. 1, p. 818–830, 1953. 12
- HINDMARSH, A. C.; GRESHO, P. M.; GRIFFITHS, D. F. The stability of explicit euler time-integration for certain finite difference approximations of the multi-dimensional advection–diffusion equation. **International Journal for Numerical Methods in Fluids**, v. 4, n. 9, p. 853–897, 1984. 27
- KUMAGAI, S.; ISODA, H. Combustion of fuel droplets in a falling chamber. **Symposium (International) on Combustion**, v. 6, n. 1, p. 726–731, 1957. 3
- KUNDU, P. K.; COHEN, I. M. **Fluid mechanics**. [S.l.: s.n.], 2004. 19, 20
- LABOWSKY, M. The effects of nearest neighbor interactions on the evaporation rate of cloud particles. **Chemical Engineering Science**, v. 31, n. 9, p. 803–813, 1976. 4
- _____. A formalism for calculating the evaporation rates of rapidly evaporating interacting particles. **Combustion Science and Technology**, v. 18, n. 3-4, p. 145–151, 1978. 4
- LAW, C. Recent advances in droplet vaporization and combustion. **Progress in Energy and Combustion Science**, v. 8, n. 3, p. 171–201, 1982. 4
- LAW, C. K. **Combustion physics**. [S.l.]: Cambridge University Press, 2006. 11

- LIÑÁN, A. The structure of diffusion flames. In: **Fluid dynamical aspects of combustion theory**. [S.l.]: Longman Scientific and Technical. 15, 16
- _____. The asymptotic structure of counterflow diffusion flames for large activation energies. **Acta Astronautica**, v. 1, n. 7-8, p. 1007–1039, 1974. 16, 22, 63
- _____. Diffusion-controlled combustion. In: AREF, H.; PHILIPS, J. (Ed.). **Mechanics for a new millenium**. [S.l.]: Kluwer Academic Publishers, 2001. p. 487–502. 15
- LIÑÁN, A.; MARTINEZ-RUIZ, D.; SÁNCHEZ, A. L.; URZAY, J. Regimes of spray vaporization and combustion in counterflow configurations. **Combustion Science and Technology**, v. 187, n. 1-2, p. 103–131, 2015. 6
- LIÑÁN, A.; MARTÍNEZ-RUIZ, D.; VERA, M.; SÁNCHEZ, A. L. The large-activation-energy analysis of extinction of counterflow diffusion flames with non-unity lewis numbers of the fuel. **Combustion and Flame**, v. 175, p. 91–106, 2017. 16
- LIÑÁN, A.; WILLIAMS, F. A. **Fundamental aspects of combustion**. [S.l.]: Oxford University Press, 1993. 15
- MAIONCHI, D.; FACHINI, F. A simple spray–flamelet model: influence of ambient temperature and fuel concentration, vaporisation source and fuel injection position. **Combustion Theory and Modelling**, v. 17, p. 522–542, 2013. 6
- MARBERRY, M.; RAY, A.; LEUNG, K. Effect of multiple particle interactions on burning droplets. **Combustion and Flame**, v. 57, n. 3, p. 237–245, 1984. 4
- MIKAMI, M.; KATO, H.; SATO, J.; KONO, M. Interactive combustion of two droplets in microgravity. **Symposium (International) on Combustion**, v. 25, n. 1, p. 431–438, 1994. 6
- MIKAMI, M.; KONO, M.; SATO, J.; DIETRICH, D. L. Interactive effects in two-droplet combustion of miscible binary fuels at high pressure. **Symposium (International) on Combustion**, v. 27, n. 2, p. 2643–2649, 1998. 6
- MIYASAKA, K.; LAW, C. K. Combustion of strongly-interacting linear droplet arrays. **Symposium (International) on Combustion**, v. 18, n. 1, p. 283–292, 1981. 6
- NAYAGAM, V.; HAGGARD, J.; COLANTONIO, R.; MARCHESE, A.; DRYER, F.; ZHANG, B.; WILLIAMS, F. A. Microgravity n-heptane droplet combustion in

oxygen-helium mixtures at atmospheric pressure. **AIAA**, v. 36, n. 8, p. 1369–1378, 1998. 3

PETERS, N. Local quenching due to flame stretch and non-premixed turbulent combustion. **Combustion Science and Technology**, v. 30, n. 1-6, p. 1–17, 1983. 16, 21, 22, 34

_____. Laminar diffusion flamelet models in non-premixed turbulent combustion. **Progress in Energy and Combustion Science**, v. 10, p. 319–339, 1984. 21

PROTTER, M. H.; WEINBERGER, H. F. **Maximum principles in differential equations**. [S.l.]: Springer Science & Business Media, 2012. 17

SÁNCHEZ, A. L.; URZAY, J.; LIÑÁN, A. The role of separation of scales in the description of spray combustion. **Proceedings of the Combustion Institute**, v. 35, n. 2, p. 1549–1577, 2015. 4

SANGIOVANNI, J.; KESTEN, A. Effect of droplet interaction on ignition in monodispersed droplet streams. **Symposium (International) on Combustion**, v. 16, n. 1, p. 577–592, 1977. 6

SANGIOVANNI, J.; LABOWSKY, M. Burning times of linear fuel droplet arrays: a comparison of experiment and theory. **Combustion and Flame**, v. 47, p. 15–30, 1982. 5

SAZHIN, S. Advanced models of fuel droplet heating and evaporation. **Progress in Energy and Combustion Science**, v. 32, n. 2, p. 162–214, 2006. 6

SILVERMAN, I.; SIRIGNANO, W. Multi-droplet interaction effects in dense sprays. **International Journal of Multiphase Flow**, v. 20, n. 1, p. 99–116, 1994. 5

SIRIGNANO, W. A. Fuel droplet vaporization and spray combustion theory. **Progress in Energy and Combustion Science**, v. 9, n. 4, p. 291–322, 1983. 4

_____. Advances in droplet array combustion theory and modeling. **Progress in Energy and Combustion Science**, v. 42, p. 54–86, 2014. 4, 5

SPALDING, D. B. The combustion of liquid fuels. **Symposium (International) on Combustion**, v. 4, n. 1, p. 847–864, 1953. 12

STRUK, P. M.; DIETRICH, D. L.; IKEGAMI, M.; XU, G. Interacting droplet combustion under conditions of extinction. **Proceedings of the Combustion Institute**, v. 29, n. 1, p. 609–615, 2002. 6

- TSAI, J.; STERLING, A. M. The combustion of a linear droplet array in a convective, coaxial potential flow. **Combustion and Flame**, v. 86, n. 3, p. 189–202, 1991. 5, 6
- _____. The combustion of linear droplet arrays. **Symposium (International) on Combustion**, v. 23, n. 1, p. 1405–1411, 1991. 5
- TWARDUS, E. M.; BRZUSTOWSKI, T. A. The interaction between two burning fuel droplets. **Archiwum Termodynamiki i Spalania**, v. 8, n. 3, p. 347–358, 1977. 4
- UMEMURA, A. Interactive droplet vaporization and combustion: approach from asymptotics. **Progress in Energy and Combustion Science**, v. 20, n. 4, p. 325–372, 1994. 5
- UMEMURA, A.; OGAWA, S.; OSHIMA, N. Analysis of the interaction between two burning droplets. **Combustion and Flame**, v. 41, p. 45–55, 1981. 4
- WALDMAN, C. H. Theory of non-steady state droplet combustion. **Symposium (International) on Combustion**, v. 15, p. 429–441, 1975. 13
- WILLIAMS, F. A. On the assumptions underlying droplet vaporization and combustion theories. **Journal of Chemical Physics**, v. 33, p. 133–144, 1960. 6
- _____. **Combustion theory**. [S.l.]: The Benjamin/Cummings, 1985. 11

APPENDIX A - AN ALTERNATIVE DERIVATION OF THE BOUNDARY CONDITIONS AT THE DROPLET SURFACE

In order to obtain the boundary conditions at the droplet surface, the equations need to be integrated in the region $0 < R \leq a$, in which a is the nondimensional droplet radius. To account for the transient variation due to phase change in the droplet surface, the generic property Φ is written as

$$\Phi(R, t) = (\Phi_g - \Phi_l)\mathcal{H}(R - a(t)) + \Phi_l, \quad 0 < R \leq a, \quad (\text{A.1})$$

in which Φ_g and Φ_l are the values of Φ in the gaseous and liquid phases, respectively, and \mathcal{H} is the Heaviside step function, here defined as

$$\mathcal{H}(R) := \begin{cases} 0, & R < 0, \\ 1, & R \geq 0. \end{cases} \quad (\text{A.2})$$

The derivative of Φ in relation to time can be obtained with the chain rule as

$$\frac{\partial \Phi}{\partial t} = -(\Phi_g - \Phi_l) \frac{da}{dt} \delta(R - a(t)) \quad 0 < R \leq a, \quad (\text{A.3})$$

in which δ is the Dirac delta function. From the sifting property of the Dirac delta function, one has

$$\int_0^a \frac{\partial \Phi}{\partial t} R^2 dR = -(\Phi_g - \Phi_l) a^2 \frac{da}{dt} = \lambda(\Phi_g - \Phi_l), \quad (\text{A.4})$$

in which $\lambda = -a^2 da/dt$ is the nondimensional vaporization rate. This identity can be applied to each conservation equation to obtain the boundary conditions.

Integrating the continuity equation in $0 < R \leq a$, one has

$$\epsilon \int_0^a \frac{\partial \rho}{\partial t} R^2 dR + (R^2 \rho U)_0^a = 0. \quad (\text{A.5})$$

From Eq. (A.4), using $\Phi = \rho$, $\Phi_l = \epsilon$ and $\Phi_g = \rho$, the first term is $\lambda(\epsilon - 1) \approx -\lambda$, since $\epsilon \ll 1$, leading finally to

$$U = \frac{\lambda}{\rho a^2}, \quad R = a. \quad (\text{A.6})$$

Applying the same procedure to the energy conservation equation, one has

$$\epsilon \int_0^a \frac{\partial(\rho c_p T)}{\partial t} R^2 dR + \lambda T = a^2 \frac{\partial T}{\partial R}, \quad (\text{A.7})$$

which leads to

$$\lambda((\epsilon + 1)T - c_{pl}T_b) = a^2 \frac{\partial T}{\partial R}. \quad (\text{A.8})$$

The left-hand side term, which is approximately $\lambda(T - c_{pl}T_b)$, is the difference between the specific heat of the gaseous and the liquid phase, which is λl , being $l = \hat{l}/\hat{c}_{p\infty}\hat{T}_\infty$ the nondimensional latent heat of vaporization, which leads to

$$a^2 \frac{\partial T}{\partial R} = \lambda l, \quad R = a. \quad (\text{A.9})$$

Similarly, for the fuel conservation equation,

$$\epsilon \int_0^a \frac{\partial(\rho Y_F)}{\partial t} R^2 dR + \lambda Y_F = \frac{1}{Le_F} a^2 \frac{\partial Y_F}{\partial R}. \quad (\text{A.10})$$

Using $Y_F = 1$ inside the droplet,

$$\frac{1}{Le_F} a^2 \frac{\partial Y_F}{\partial R} - \lambda Y_F = (\epsilon Y_F - 1)\lambda, \quad (\text{A.11})$$

which can be approximated as

$$\frac{1}{Le_F} a^2 \frac{\partial Y_F}{\partial R} - \lambda Y_F = -\lambda, \quad R = a. \quad (\text{A.12})$$

APPENDIX B - THE ASYMPTOTIC STRUCTURE OF DIFFUSION FLAMES

The conservation equations in the flame are

$$\frac{d^2 T}{dZ^2} = -q \frac{2}{\chi_f} Da y_O y_F \exp \left[\frac{T_a}{T_f} \left(1 - \frac{T_f}{T} \right) \right], \quad (3.88)$$

$$\frac{d^2 y_O}{dZ^2} = s_Z \frac{2}{\chi_f} Da y_O y_F \exp \left[\frac{T_a}{T_f} \left(1 - \frac{T_f}{T} \right) \right], \quad (3.89)$$

$$\frac{d^2 y_F}{dZ^2} = \frac{2}{\chi_f} Da y_O y_F \exp \left[\frac{T_a}{T_f} \left(1 - \frac{T_f}{T} \right) \right]. \quad (3.90)$$

The variables are expanded in a perturbation series around their values at the flame as

$$Z = 1 + \varepsilon \frac{A_\zeta}{\delta^{1/3}} \zeta, \quad (B.1)$$

$$T = T_f - \varepsilon \frac{1}{\delta^{1/3}} (\theta + \gamma \zeta) + O(\varepsilon^2), \quad (B.2)$$

$$y_O = 0 + \varepsilon \frac{A_\zeta}{\delta^{1/3}} \Psi_O + O(\varepsilon^2), \quad (B.3)$$

$$y_F = 0 + \varepsilon \frac{A_\zeta}{\delta^{1/3}} \Psi_F + O(\varepsilon^2), \quad (B.4)$$

in which ζ is the independent variable in the flame scale, δ is the reduced Damköhler number, ε is the perturbation parameter (unrelated to the ratio between densities ϵ), A_ζ and γ are constants and θ , Ψ_F and Ψ_O are the perturbations in the temperature and fuel and oxidizer concentrations, respectively. The role of the term $\gamma \zeta$ in the expansion of the temperature is to normalize the gradients of the perturbation θ .

Substituting the expansions in Eqs. (3.88), (3.89) and (3.90) and neglecting higher order terms leads to

$$\frac{d^2 \theta}{d\zeta^2} = \frac{q}{s_Z} \frac{d^2 \Psi_O}{d\zeta^2} = q \frac{d^2 \Psi_F}{d\zeta^2} = \frac{2}{\chi_f} q \frac{A_\zeta^3 \varepsilon^3}{\delta} Da \Psi_O \Psi_F \exp \left[\frac{T_a}{T_f} \left(1 + \frac{T_f}{\varepsilon \frac{1}{\delta^{1/3}} (\theta + \gamma \zeta)} \right)^{-1} \right] \quad (B.5)$$

Expanding the argument of the exponential as a Taylor series around $\varepsilon = 0$ and

neglecting the higher order terms leads to

$$\frac{d^2\theta}{d\zeta^2} = \frac{q}{S} \frac{d^2\Psi_O}{d\zeta^2} = q \frac{d^2\Psi_F}{d\zeta^2} = \frac{2}{\chi_f} q \frac{A_\zeta^3 \varepsilon^3}{\delta} Da \Psi_O \Psi_F \exp \left[-\frac{T_a}{T_f^2} \frac{\varepsilon}{\delta^{1/3}} (\theta + \gamma\zeta) \right]. \quad (\text{B.6})$$

This expression suggests that $\varepsilon = T_f^2/T_a$ is the suitable choice for the perturbation parameter to address the influence of the activation temperature and the flame temperature over the extinction. Therefore, one has

$$\frac{d^2\theta}{d\zeta^2} = \frac{q}{s_Z} \frac{d^2\Psi_O}{d\zeta^2} = q \frac{d^2\Psi_F}{d\zeta^2} = \left(\frac{2}{\chi_f} q \frac{A_\zeta^3 \varepsilon^3}{\delta} Da \right) \Psi_O \Psi_F \exp \left(-\frac{\theta + \gamma\zeta}{\delta^{1/3}} \right). \quad (\text{B.7})$$

The solution in the Burke-Schumann region is utilized to provide the boundary conditions to the inner solution through the fluxes of the properties in the flame, i.e.,

$$T'^+ := \left. \frac{dT}{dZ} \right|_{Z=1^+} = -\frac{\delta^{1/3}}{\varepsilon A_\zeta} \frac{\varepsilon}{\delta^{1/3}} \frac{d}{d\zeta} (\theta + \gamma\zeta) \Big|_{\infty} = -\frac{1}{A_\zeta} \left(\left. \frac{d\theta}{d\zeta} \right|_{\infty} + \gamma \right), \quad (\text{B.8})$$

$$T'^- := \left. \frac{dT}{dZ} \right|_{Z=1^-} = -\frac{\delta^{1/3}}{\varepsilon A_\zeta} \frac{\varepsilon}{\delta^{1/3}} \frac{d}{d\zeta} (\theta + \gamma\zeta) \Big|_{-\infty} = -\frac{1}{A_\zeta} \left(\left. \frac{d\theta}{d\zeta} \right|_{-\infty} + \gamma \right), \quad (\text{B.9})$$

In order to set $d\theta/d\zeta|_{\infty} = 1$ and $d\theta/d\zeta|_{-\infty} = -1$, for simplicity, one has

$$\gamma + A_\zeta T'^- = 1, \quad (\text{B.10})$$

$$\gamma + A_\zeta T'^+ = -1, \quad (\text{B.11})$$

which is satisfied by

$$\gamma = \frac{T'^+ + T'^-}{T'^+ - T'^-}, \quad A_\zeta = -\frac{2}{T'^+ - T'^-}. \quad (\text{B.12})$$

Subtracting the conservation equations from each other leads to the following relation

$$q A_\zeta \frac{d^2\Psi_F}{d\zeta^2} - \frac{d^2\theta}{d\zeta^2} = 0, \quad \frac{q A_\zeta}{s_Z} \frac{d^2\Psi_O}{d\zeta^2} - \frac{d^2\theta}{d\zeta^2} = 0, \quad (\text{B.13})$$

that, integrated once, leads to

$$qA_\zeta \frac{d\Psi_F}{d\zeta} - \frac{d\theta}{d\zeta} = C_1, \quad \frac{qA_\zeta}{s_Z} \frac{d\Psi_O}{d\zeta} - \frac{d\theta}{d\zeta} = C_2. \quad (\text{B.14})$$

Using the conditions at $\zeta \rightarrow -\infty$ and $\zeta \rightarrow \infty$, respectively, provide $C_1 = -1$ and $C_2 = 1$. Integrating again, one has

$$qA_\zeta \Psi_F - \theta = -\zeta, \quad \frac{qA_\zeta}{s_Z} \Psi_O - \theta = \zeta, \quad (\text{B.15})$$

which allows Ψ_F and Ψ_O to be written as

$$\Psi_F = \frac{1}{qA_\zeta}(\theta - \zeta), \quad \Psi_O = \frac{s_Z}{qA_\zeta}(\theta + \zeta). \quad (\text{B.16})$$

Thus, defining

$$\delta := \frac{4}{\chi_f} \frac{\varepsilon^3 s_Z Da}{q(T'^- - T'^+)}, \quad (\text{B.17})$$

the Eq. (3.88) can be written as

$$\frac{d^2\theta}{d\zeta^2} = (\theta + \zeta)(\theta - \zeta) \exp\left(-\frac{\theta + \gamma\zeta}{\delta^{1/3}}\right), \quad (\text{B.18})$$

with boundary conditions

$$\left. \frac{d\theta}{d\zeta} \right|_{\infty} = 1, \quad \left. \frac{d\theta}{d\zeta} \right|_{-\infty} = -1. \quad (\text{B.19})$$

This form of the energy conservation equation is known as canonical form, and was originally studied by Liñán in the analysis of diffusion flame extinction (LIÑÁN, 1974). It was shown that, for given γ , there is a δ for which below it there is no valid solution to the equation, which represents the extinction of the flame. An approximated expression for this critical value of δ as a function of γ is (LIÑÁN, 1974)

$$\delta_E = e[(1 - |\gamma|) - (1 - |\gamma|)^2 + 0.26(1 - |\gamma|)^3 + 0.055(1 - |\gamma|)^4]. \quad (\text{B.20})$$

PUBLICAÇÕES TÉCNICO-CIENTÍFICAS EDITADAS PELO INPE

Teses e Dissertações (TDI)

Teses e Dissertações apresentadas nos Cursos de Pós-Graduação do INPE.

Manuais Técnicos (MAN)

São publicações de caráter técnico que incluem normas, procedimentos, instruções e orientações.

Notas Técnico-Científicas (NTC)

Incluem resultados preliminares de pesquisa, descrição de equipamentos, descrição e ou documentação de programas de computador, descrição de sistemas e experimentos, apresentação de testes, dados, atlas, e documentação de projetos de engenharia.

Relatórios de Pesquisa (RPQ)

Reportam resultados ou progressos de pesquisas tanto de natureza técnica quanto científica, cujo nível seja compatível com o de uma publicação em periódico nacional ou internacional.

Propostas e Relatórios de Projetos (PRP)

São propostas de projetos técnico-científicos e relatórios de acompanhamento de projetos, atividades e convênios.

Publicações Didáticas (PUD)

Incluem apostilas, notas de aula e manuais didáticos.

Publicações Seriadas

São os seriados técnico-científicos: boletins, periódicos, anuários e anais de eventos (simpósios e congressos). Constam destas publicações o Internacional Standard Serial Number (ISSN), que é um código único e definitivo para identificação de títulos de seriados.

Programas de Computador (PDC)

São a seqüência de instruções ou códigos, expressos em uma linguagem de programação compilada ou interpretada, a ser executada por um computador para alcançar um determinado objetivo. Aceitam-se tanto programas fonte quanto os executáveis.

Pré-publicações (PRE)

Todos os artigos publicados em periódicos, anais e como capítulos de livros.